REVERSE OSMOSIS

1. Introduction

Reverse osmosis (RO) is a fairly mature technology that has been applied to a wide range of separation–recovery processes (1). The ever-expanding market for RO processes is the result of significant advances both in the development of thin-film composite membranes (2) and the ability to minimize process problems caused by fouling of the membrane surface (3). The origins of RO can be traced back to the late 1950s where the work of Reid showed that cellulose acetate RO membranes were capable of separating salt from water, even though the water fluxes obtained were too small to be practical (4–7). Then, in the early 1960s, Loeb and Sourirajan developed a method for making asymmetric cellulose acetate membranes with relatively high water fluxes and separations, thus making RO separations both possible and practical (8–10).

Since then, the development of new-generation membranes that can withstand harsher operating conditions (wider pH ranges, higher temperatures, etc) while maintaining far superior water flux and solute separation characteristics has helped push RO to the forefront of separation processes. The evolution of hybridized processes that combine RO with other conventional separation technologies like ultra- and nanofiltration (loose RO), distillation, or crystallization has led to a much broader range of applications (3). Beyond the traditional seawater and brackish water desalination processes, RO membranes have found uses in wastewater treatment, production of ultrapure water, water softening, food processing, pharmaceutical recovery, as well as many others (1,11,12). Perhaps the greatest indication of the acceptance of RO processes is the market growth over the past 15 years. In 1990, the entire RO market was $118 million (13). A recent estimate indicates that sales of RO membrane products just in the area of desalination grew to $1.1 billion in 2003, with a potential market of $1.8 billion by 2007 (14).

The driving force for the development and use of RO membranes is the advantages that these have over traditional separation processes, such as distillation, extraction, ion exchange, and adsorption. Reverse osmosis is a pressure-driven process so no energy-intensive phase changes or potentially expensive solvents or adsorbents are needed for RO separations. Reverse osmosis is a process that is inherently simple to design and operate compared to many traditional separation processes. Also, simultaneous separation and concentration of both inorganic and organic compounds is possible with the RO process. In addition, with nanofiltration (NF) membranes selective solute separations based on charge and molecular weight–size differences are possible. Excellent reviews of RO technology and theories have been reported in the literature by Parekh (15), Belfort (16), Sourirajan and Matsuura (10), Lloyd and Meluch (17), Bhattacharyya and co-workers (11), Rautenbach and Albrecht (18), Howell and co-workers (19), and Riley (13).

2. RO Membrane Materials and Modules

Reverse osmosis membrane separations are, most importantly, governed by the properties of the membrane used in the process. These properties depend on the chemical nature of the membrane material (almost always a polymer) as well as its physical structure. Properties for the ideal RO membrane include resistance to chemical and microbial attack, mechanical, and structural stability over long operating periods, and the desired separation characteristics for each particular system. However, few membranes satisfy all these criteria and so compromises must be made to select the best RO membrane available for each application. Excellent discussions of typical RO membrane materials, preparation methods, and structures include Kesting (20), Lloyd and Meluch (17), Cabasso (21), Koros and co-workers (22), Baker (23), Strathmann (24), Petersen and Cadotte (25), and Petersen (2).

Most currently available RO membranes fall into two categories: asymmetric membranes containing one polymer, and thin-film composite (TFC) membranes consisting of two or more polymer layers. Asymmetric RO membranes have a very thin, permselective skin layer supported on a more porous sublayer of the same polymer; the dense skin layer determines the fluxes and selectivities of these membranes while the porous sublayer serves only as a mechanical support for the skin layer and has little effect on the membrane separation properties. Asymmetric membranes are most commonly formed by a phase inversion (polymer precipitation) process (20). In this process, a polymer solution is precipitated into a polymer-rich solid phase that forms the membrane and a polymer-poor liquid phase that forms the membrane pores or void spaces.

An excellent review of composite RO and NF membranes has been reported by Petersen (2). Thin-film, composite membranes consist of a thin polymer barrier layer formed on one or more porous support layers (almost always a different polymer from the surface layer). The surface layer determines the flux and separation characteristics of the membrane; the porous backing serves only as a support for the barrier layer and so has almost no effect on membrane transport properties. The barrier layer is extremely thin, thus allowing high water fluxes. The most important TF, composite membranes are made by interfacial polymerization, a process in which a highly porous membrane (usually polysulfone) is coated with a polymer or monomer and then reacted with a cross-linking agent.

Although RO membranes have been formed and tested with a wide range of different materials and preparation techniques, the cellulosic polymers [cellulose acetate (CA), cellulose triacetate, etc], linear and cross-linked aromatic polyamide, and aryl–alkyl polyetherurea are among the most important RO membrane materials (2,13,24). Asymmetric cellulose acetate membranes continue to enjoy widespread use despite some disadvantages: a narrow pH operating range (4.5–7.5) since it is subject to hydrolysis; susceptibility to biological attack; compaction (mechanical compression) at high pressures that results in reduced water flux; and low upper temperature limits (~35°C). Polyamide and polyurea composite membranes typically have higher water fluxes and salt and organic rejections, can withstand higher temperature and larger pH variations

(4−11 pH), and are immune to biological attack and compaction. However, these membranes tend to be less chlorine resistant and more susceptible to oxidation compared to cellulose acetate membranes. Figure 1 shows water flux and NaCl rejections for three different classes of commercially available RO membranes [Seawater (SWRO), Brackish water (BWRO), and Low Pressure/Other Applications] made from a variety of polymer materials. Bhattacharyya and co-workers (11) also list selected solute (both inorganic and organic) rejections for a large number of RO membranes. Responding to the rising demand, GE Osmonics (among others) has introduced a special class of composite membranes developed for applications involving highly acidic environments. The membranes, developed for both RO and NF applications can remain stable even at pH 1. Some characterisitics of these films are given in Table 1.

State-of-the-art analytical techniques, such as atomic force microscopy (AFM), have led to significant breakthroughs in understanding the impact of the polymer on membrane performance. For example, it is well known that the solute separation characteristics of RO/NF membranes are greatly affected by the swelling of the polymer in the presence of a solvent. To better understand how the two attributes are related, Freger (26) was able to use AFM to provide an excellent insight into the impact of swelling under various conditions on the separation behavior of commercially available polyamide TFC RO and NF membranes. The NF membranes showed a decline in water flux with increasing salinity, which could not be accounted for by using the concept of concentration polarization (see below). However, using AFM they were able to quantify the degree of swelling for the membranes in solutions of varying salinity and found that swelling decreased with increasing salinity. Since permeability increases with swelling, the observed change in flux could be attributed to membrane swelling. Similar experiments examining RO membranes showed no significant swelling of the fully aromatic polyamide network. This work is rather significant since it is the first to demonstrate an effective technique for quantifying the true thickness of the selective skin layer. Hilal and co-workers (27) used AFM to characterize the surface of NF membranes to help understand the impact of pore size distribution, surface charge, and surface morphology on NF separations. Kwak and co-workers (28) used AFM to study the effects of additives on water flux through polyamide TFC membranes containing the commercially used cross-linker dimethyl sulfoxide (DMSO). They were able to show that the larger flux is caused by increased surface roughness (larger surface area for transport) resulting from the incorporation of DMSO into the polymer matrix.

The evolution of nanotechnology has also influenced the realm of RO−NF separations. To combat the problem of biofilm formation (fouling), Kwak and co-workers (29) developed a new polyamide film containing self-assembled 2-nm TiO_2 nanoparticles, since TiO_2 is a known photocatalyst that can be used to kill bacteria. Preliminary laboratory experiments examined the ability of the membranes under ultraviolet (uv) exposure to destroy *Escherichia Coli* colonies growing on the surface, with complete sterilization being achieved within 4 h. As significant as these results are, the need for a uv light source presents a major obstacle to practical application of this type of technology for large-scale field applications.

While the membrane material largely determines the water and solute fluxes in a RO process, the packaging of the RO membrane is also extremely important for process feasibility. The requirements of a membrane module include (*1*) that it offer mechanical support to the RO membrane even at high operating pressures (up to 80 bar); (*2*) that the design minimize pressure drop across the module as well as fouling and concentration polarization; and (*3*) that the module be relatively inexpensive and easy to replace in the membrane process. The most common commercially available membrane modules include plate-and-frame, tubular, spiral-wound, and hollow-fiber elements. For large-scale desalination applications, spiral-wound modules have been commonly used. Another type of membrane module (Disc Tube) with reduced fouling problems, has been applied to various environmental problems ranging in sizes from 10 to 2000 m^3/day (30,31). An in-depth review of the recent advances in module design has been given by Drioli and Romano (12). Marriott and Sorensen (32) developed a general approach for modeling transport processes in hollow-fiber and spiral-wound modules.

The most significant constraint affecting module design today is increasing demand for minimal floorspace within a plant. Therefore, the key factor to consider when designing an RO system is module size since several sizes are sold commercially. The typical RO unit consists of a network of several 8 (0.203 m) × 40 (1.012 m)-in. spiral wound modules, or elements (Fig. 2). A 3800-m^3/day system using this size element would require 175 elements. The recently developed MegaMagnum RO element (Koch Membrane Systems, Inc.) is an 18 (0.4572 m) × 61 (1.5494 m)-in. spiral wound module that is designed to provide maximum membrane area while still being practical to physically handle. To produce the same 3800 m^3/day, only 25 MegaMagnum elements would be needed, occupying 50% less floorspace (33). These types of advances are the driving forces behind the spread of RO–NF tecnology.

3. Theoretical Aspects

A reverse osmosis membrane acts as the semipermeable barrier to flow in the RO process, allowing selective passage of a particular species (usually water) while partially or completely retaining other species (solutes, such as salts). Chemical potential gradients across the membrane provide the driving forces for solute and solvent transport across the membrane: $-\Delta\mu_s$, the solute chemical potential gradient, is usually expressed in terms of concentration; and $-\Delta\mu_w$, the water (solvent) chemical potential gradient, is usually expressed in terms of pressure difference across the membrane.

3.1. Measurable Process Parameters. The RO process is relatively simple in design. It consists of a feed water source, feed pretreatment, high pressure pump, RO membrane modules, and, in some cases, posttreatment steps. A schematic of the simplified RO process is shown in Fig. 3**a**.

The three streams (and associated variables) of the RO membrane process are shown in Fig. 3**b**: the feed; the product or permeate stream; and the concentrated feed stream, called the concentrate or retentate. The water flow through the membrane is reported in terms of water flux, J_w, where

$$J_\mathrm{w} = \frac{\text{volumetric or mass permeation rate}}{\text{membrane area}}$$

Solute passage is defined in terms of solute flux, J_s:

$$J_\mathrm{s} = \frac{\text{mass permeation rate}}{\text{membrane area}}$$

Solute separation is measured in terms of observed rejection, R, defined as

$$R = 1 - \frac{C_\mathrm{P}}{C_\mathrm{F}} \tag{1}$$

The quantity of feed water that passes through the membrane (the permeate) is measured in terms of water recovery, r, defined for a batch RO system as

$$r = \frac{\Sigma J_\mathrm{w} A_\mathrm{m} \Delta t}{V_\mathrm{F}} = \frac{V_\mathrm{P}}{V_\mathrm{F}} \tag{2}$$

and for a continuous system as

$$r = \frac{J_\mathrm{w} A_\mathrm{m}}{F_\mathrm{F}} = \frac{F_\mathrm{P}}{F_\mathrm{F}} \tag{3}$$

In a batch membrane system, water is recovered from the system as the concentrate (retentate) is recycled to the feed tank; as a result, if the solute is rejected the feed concentration (C_F) continuously increases over time. For a continuous membrane system, fresh feed is continuously supplied to the membrane.

Water flux is sometimes normalized relative to the initial or pure water flux (J_wo) as $J_\mathrm{w}/J_\mathrm{wo}$, or as flux drop, defined by

$$\text{Flux drop} = 1 - \frac{J_\mathrm{w}}{J_\mathrm{wo}} \tag{4}$$

The pressure difference between the high and low pressure sides of the membrane is denoted as ΔP while the osmotic pressure difference across the membrane is defined as $\Delta\pi$; the net driving force for water transport across the membrane is $(\Delta P - \sigma\Delta\pi)$, where σ is the Staverman reflection coefficient ($\sigma = 1$ means 100% solute rejection). Gekas (34) reviewed the standardized terminology recommended for use to describe pressure-driven membrane processes, including for reverse osmosis.

3.2. Transport Models. Many mechanistic and mathematical models have been proposed to describe reverse osmosis membranes. Some of these descriptions rely on relatively simple concepts, while others are far more complex and require sophisticated solution techniques. Models that adequately describe the performance of RO membranes are very important since these are needed in the design of RO processes. Models that predict separation characteristics also minimize the number of experiments that must be performed to describe a particular system. Classic reviews of membrane transport models and mechanisms include Jonsson (35), Soltanieh and Gill (36), Mazid (37), Pusch (38), Dickson (39), Rautenbach and Albrecht (18), and Bhattacharyya and co-workers (11).

Reverse osmosis models can be divided into three types: irreversible thermodynamics models (eg, Kedem-Katchalsky and Spiegler-Kedem models); nonporous or homogeneous membrane models [eg, the solution-diffusion (SD), solution-diffusion-imperfection, and extended solution-diffusion models]; and pore models (eg, the finely porous, preferential sorption-capillary flow, and surface force-pore flow models). The transport models focus on the top thin skin of asymmetric membranes or the top thin skin layer of composite membranes since these determine fluxes and selectivities of most membranes. Also, most of the membrane models assume equilibrium (or near equilibrium) or steady-state conditions in the membrane.

A fundamental difference exists between the assumptions of the homogeneous and porous membrane models. The homogeneous models assume that the membrane is nonporous; ie, transport takes place between the interstitial spaces of the polymer chains or polymer nodules, usually by diffusion. The porous models assume that transport takes place through pores that run the length of the membrane barrier layer; as a result, transport can occur by both diffusion and convection through the pores. While both conceptual models have had some success in predicting RO separations, the question of whether a RO membrane is truly homogeneous (no pores) or porous is still a point of debate. There is no technique currently available to definitively answer this question. For the sake of brevity, two models (nonporous, diffusion-based model, and pore-based model) will be discussed here.

3.3. Solution-Diffusion Model. The model assumes that: (*1*) the RO membrane has a homogeneous, nonporous surface layer; (*2*) both the solute and solvent dissolve in this layer and then each diffuses across it; (*3*) the solute and solvent diffusion is uncoupled and due to its own chemical potential gradient across the membrane; (*4*) these gradients are the result of concentration and pressure differences across the membrane (36,39). The driving force for water transport is primarily due to the net transmembrane pressure difference and can be represented by

$$J_{\mathrm{w}} = \frac{D_{\mathrm{wm}} C_{\mathrm{wm}} \overline{V}_{\mathrm{w}}}{R_{\mathrm{g}} T \delta} (\Delta P - \Delta \pi) \equiv A(\Delta P - \Delta \pi) \tag{5}$$

where A is termed the water permeability coefficient.

For the solute flux it is assumed that chemical potential difference due to pressure is negligible and so the driving force is almost entirely due to concentration differences. The solute flux equation is

$$J_{\mathrm{s}} = \frac{D_{\mathrm{sm}} K_{\mathrm{sm}}}{\delta} (C_{\mathrm{wall}} - C_{\mathrm{P}}) \equiv B(C_{\mathrm{wall}} - C_{\mathrm{P}}) \tag{6}$$

where B is referred to as the solute permeability coefficient. In the absence of concentration polarization, C_{wall} can be replaced by either C_{B} (bulk solute conc) or by C_F (feed conc for negligible water recovery) in equation 6. By using the relations for solvent and solute flux, solute rejection for the SD model can be expressed as

$$\frac{1}{R} = 1 + \left(\frac{B}{A}\right)\left(\frac{1}{\Delta P - \Delta\pi}\right) \tag{7}$$

Equation 7 shows that as $\Delta P \rightarrow \infty$, $R \rightarrow 1$. The principal advantage of the SD model is that only two parameters are needed to characterize the membrane system. As a result, it has been widely applied to both inorganic salt and organic solute systems. However, Soltanieh and Gill (36) indicated that the SD model is limited to membranes with low water content. They and Mazid (37) also have pointed out that for many RO membranes and solutes, particularly organics, the SD model does not adequately describe water or solute flux. They discuss possible causes for these deviations as suggested by other researchers, including imperfections in the membrane barrier layer, pore flow (convection effects), and solute–solvent–membrane interactions.

Burghoff and co-workers (40) recognized that the SD model does not explain the negative solute rejections found for some organics and so formulated the extended-solution-diffusion model. They pointed out that the SD model does not take into account possible pressure dependence of the solute chemical potential which, while negligible for inorganic salt solutions, can be important for organic solutes (38,41). Recently, Paul (42) presented an excellent review and reformulation of the classical solution-diffusion model to allow its application to all types of systems. Specifically, he attacks the problem using a rigorous multicomponent diffusion formalism based on the irreversible thermodynamic Maxwell-Stefan equations. His approach can even be used to account for breakdowns in traditional SD theory related to coupled solute–solvent transport (ie, negative rejections).

3.4. Surface Force-Pore Flow Model. The surface force-pore flow (SFPF) model developed by Sourirajan and Matsuura (10,43) is a two-dimensional (2D) extension of the finely porous model. While the finely porous model considers only axial solute concentration gradients, the SFPF model recognizes that the solute concentration in a RO membrane pore may be a function of radial as well as axial position (41). The SFPF model assumes: (*1*) water transport through the membrane occurs in pores by viscous flow; (*2*) solute transport takes place by diffusion and convection in the membrane pores; (*3*) transport of both water and solute through the membrane pores is determined by interaction forces, friction forces, and chemical potential gradients of the water and solute; (*4*) the pores of the membrane are cylindrical and run the length of the membrane barrier layer; (*5*) a molecular layer of pure water is preferentially sorbed on the pore wall; and (*6*) a potential field controls the solute distribution of the membrane pore. An important modification of the SFPF model has been formulated to recognize that it is more realistic to assume a distribution of membrane pore sizes. Mehdizadeh and Dickson (44) and Mehdizadeh (45) also pointed out some inconsistencies in the SFPF model similar to those pointed out for the original finely porous model; they formulated a modified SFPF correcting these conceptual errors. The SFPF models required the solution of velocity profile equation in the pore, force balance equation of solute in the pore, and correlations of interaction parameters with potential function. The pure water flow rate has been described by the Poiseuille equation.

The transport equations for the SFPF model, expressed in dimensionless form, have been solved using a variety of numerical techniques. Sourirajan and Matsuura (10) used liquid chromatography techniques in order to determine $\tilde{A}$ (measure of electrostatic repulsion force between the ionic solute and the membrane) or $\tilde{B}$ (measure of short range van der Waals forces) for a solute and then used trial and error to find the membrane pore radius: R_p (pore radius) was varied until the predicted and measured permeate concentrations were in agreement. Alternatively, if R_p was specified, then $\tilde{A}$ or $\tilde{B}$ was varied to produce agreement in the predicted and measured permeate concentrations. Mehdizadeh and Dickson (44,46) used a similar solution technique. Bhattacharyya and co-workers (47) used measured pore radius values and one experimental data point for permeate concentration, eliminated the need for trial and error solution of the transport equations. Both solution techniques indicated that the SFPF model gave excellent predictions of solute separation for a wide range of inorganics and organics under varying operating conditions. However, for some dilute organics that cause substantial decreases in water flux, the models do not adequately predict the water flux.

4. Concentration Polarization

Concentration polarization (CP) is the term used to describe the accumulation of rejected solute at the surface of a membrane so that the solute concentration at the membrane wall is much higher than that of the bulk feed solution. The enhanced solute concentration on the membrane surface causes reduction of water flux due to increased osmotic pressure (see eq. 5), precipitation of sparingly soluble salts (eg, $CaSO_4$), reduced permeate quality, etc. The experimental result (48) showing a dramatic reduction in water flux for $CaSO_4$ solution is shown in Fig. 4. The experiment was conducted in a batch system using an aromatic polyamide (FT30) RO membrane. High mixing (to prevent CP) was used for 60 min, after which the experiment was continued with no mixing. As soon as the mixing was stopped, CP increased and the wall concentration of $CaSO_4$ exceeded saturation causing very high flux drop due to precipitate formation.

Reviews of concentration polarization have been reported by Matthiasson and Sivik (49), Gekas and Hallstrom (50), and Rautenbach and Albrecht (18). Since solute wall concentration may not be experimentally measurable, models relating solute and solvent fluxes with hydrodynamic parameters are needed for system design. Bhattacharyya and co-workers (51) have numerically solved the Navier-Stokes diffusion-convection equation to calculate wall concentration, and thus water flux and permeate quality.

A simplified model using stagnant boundary-layer assumption and the one-dimension (1D) diffusion-convection equation has been used to calculate wall concentration in an RO module. The integrated form of this equation is given in equation 8.

$$\frac{C_{\mathrm{wall}} - C_{\mathrm{P}}}{C_{\mathrm{B}} - C_{\mathrm{P}}} = \exp(\frac{V_{\mathrm{w}}}{k_{\mathrm{s}}}) \tag{8}$$

This is the widely applied film theory developed by Brian (52). Gekas and Hallstrom (50) reviewed correlations for the mass transfer coefficient, k_{S} (as Sherwood number) for various membrane geometries.

By using the simplified model, one can easily perform CP simulations as a function of feed and operating variables (eg, pressure, temperature, flow rate). Consider the treatment of a 5000-mg/L NaCl solution using a tubular RO module of diameter "d" as a test case. Assume negligible water recovery, temperature = 298 K, pressure = 51 bar, and $d = 1.27 \times 10^{-2}$ m. The steady-state permeate salt concentration (C_{p}), water flux (J_{w}), membrane rejection (both intrinsic, R_{int}, and observed, R_{obs}), and concentration polarization factor ($\mathrm{CP} = C_{\mathrm{wall}}/C_{\mathrm{B}}$) can be obtained as a function of Reynold's number (*Re*) by solving the CP equation (eq. 8) along with the SD transport equations (eqs. 5 and 6) using nonlinear computational methods. For the simulation, the following data and correlations can be used (*1*) For mass transfer correlation, $\mathrm{Sh} = 0.04\ (\mathrm{Re})^{0.75}$ $(\mathrm{Sc})^{0.33}$, (*2*) Osmotic pressure follows van't Hoff's equation ($\pi = i\ C\ R_{\mathrm{g}}\ T$), (*3*) $A = 4.05 \times 10^{-7}$ (m/s) / (bar), $B = 1.30 \times 10^{-6}$ m/s, and (*4*) $\mu = 1.0 \times 10^{-3}$ $\mathrm{kg.m^{-1}.s^{-1}}$, NaCl diffusivity in water = 1.6×10^{-9} $\mathrm{m^2/s}$, and density of solution, $\rho = 1000$ $\mathrm{kg/m^3}$. The expected increase in CP with decreasing Re is shown in Fig. 5**a**. The effect of feed flow rate on NaCl rejection (R_{int} and R_{obs}) is shown in Fig. 5**b**. Since intrinsic rejection ($R_{\mathrm{int}} = 1 - C_{\mathrm{P}} / C_{\mathrm{wall}}$) is defined in terms of wall concentration, it should be independent of *R*e. On the other hand, as C_{wall} increases C_{P} should increase and thus one would expect the observed rejection to be a strong function of feed flow rate. Of course, note that the maximum flowrate that can be used to minimize CP is controlled by the membrane-module pressure drop. The effects of spacers, complex flow patterns, types of fluids, etc, on CP behavior have been reported in the literature (51).

5. Study of RO Variables and Typical Experimental Setup

Factors affecting RO membrane separations and water flux include feed variables, eg, solute concentration, temperature, pH, and pretreatment requirements; membrane variables, eg, polymer type, module geometry, and module arrangement; and process variables, eg, feed flow rate, operating pressure, operating time, and water recovery.

For simple noninteracting inorganic salts, one can easily predict the trends in water flux and rejection behavior (13). As predicted by most of the RO transport models (eq. 5), water flux (J_{w}) should increase linearly with the net pressure, and the temperature dependency on flux is generally of Arrhenius type. Water flux can also gradually decrease over operating time (measured in days or months of operation) due to fouling, membrane compaction, or other changes in the membrane structure. Salt rejection (eq. 7) increases with the net pressure up to an asymptotic value. For ionizable organics, the rejection of ionized species is considerably higher than the nonionized species.

The intrinsic rejection and maximum obtainable water flux of different membranes can be easily evaluated in a stirred batch system. A typical batch unit (53) using a gas tank for pressurization is shown in Fig. 6. A continuous system is needed for full-scale system design and to determine the effects of hydrodynamic variables and fouling in different module configurations. A typical lab–pilotscale unit (with computer control and on-line data acquisition) used in our laboratory is shown in Fig. 7.

6. Applications

Examples of treatment process utilizing RO technologies can be found throughout the literature. Table 2 highlights some of the key areas of use for both technologies, with desalination of seawater and brackish water by RO continuing to be the most important application worldwide (14). Several selected applications will be discussed below.

6.1. Wastewater Applications. Several advantages of the RO process that make it particularly attractive for dilute aqueous wastewater treatment include (*1*) RO systems are simple to design and operate, have low maintenance requirements, and are modular in nature, making expansion of the systems easy; (*2*) both inorganic and organic pollutants can be removed simultaneously by RO membrane processes; (*3*) RO systems allow recovery/recycle of waste process streams with no effect on the material being recovered; (*4*) RO membrane systems often require less energy and offer lower capital and operating costs than many conventional treatment systems; and (*5*) RO processes can considerably reduce the volume of waste streams so that these can be treated more efficiently and cost effectively by other processes, such as incineration or other destruction processes (63,104,105). In addition, RO systems can replace or be used in conjunction with other treatment processes such as oxidation, adsorption, stripping, or biological treatment (as well as many others) to produce a high quality product water that can be reused or discharged.

Applications that have been reported for RO processes include the treatment of organic containing wastewater, wastewater from electroplating and metal finishing, pulp and paper, mining and petrochemical, textile and food processing industries, radioactive wastewater, municipal wastewater, and contaminated groundwater (63–65,78,79,106–109). One of the newest applications involves the treatment of wastewater generated by the semiconductor industry. This particular industry generates wastewater containing large amounts of hydrofluoric acid (HF) as well as ionic impurities that render the HF solution useless. The RO membranes that allow selective permeation of HF while rejecting the ionic impurities to produce a pure HF solution that can be reused have been reported by Kulkarni and co-workers (110).

6.2. Electroplating and Metal-Finishing Process Wastewaters. In most cases, process wastewaters from the electroplating and metal-finishing industries must be treated to remove heavy metals and organics before being discharged. Recent emphasis is being placed on generating reusable wash streams to reduce water consumption since these factories typically draw their water from nearby municipal supplies (66). Reverse osmosis is ideal for this wastewater treatment for many of these operations since it allows both recovery of the heavy metals and reuse of the product water in the process. The RO process has been used in the treatment and recovery of wastewater containing nickel, copper, zinc, copper cyanide, chromium, aluminum, and gold (63–67,78,79). The EPA (68) reported the case study results for an industrial printed circuit board production plant and demonstrated the effectiveness of RO for plating salts recovery and virtual elimination of wastewater discharge.

Cellulose acetate and polyamide (FT30) membranes were used at three Japanese plating shops with nickel, chromium, and gold plating lines (69). Up to 80% water recoveries with high metal and total dissolved solids (TDS) (>95%) rejections were possible, and the product water was recycled. The RO processes were found to be cost effective in treating the wastewaters, and the compact nature of the RO system made it highly desirable to the customers because of space limitations. However, Qin and co-workers (67) did find in their studies that some commercial membranes were susceptible to failure of the polysulfone support layer, which resulted in irrecoverable loss of membrane performance. Thorsen (70) discussed the RO treatment of effluent from an electrolytic polishing process for aluminum products. The streams contained phosphoric acid and aluminum from rinse water. The DDS HR-98 membranes allowed 96–98% acid recovery (up to an acid concentration of 20%) and produced permeate water suitable for reuse. The membranes appeared to be stable to the feed even at the low pH values (0.9–1.0) found at high recoveries.

6.3. Radioactive Processing Wastewaters. Because of high rejection of inorganic compounds, RO membranes have been studied for treatment of radioactive effluents. The RO membranes have been used to treat uranium conversion process effluent containing toxic, corrosive, and radioactive compounds (71). The FT30 membranes studied had rejections of uranium of 99.5% for water recoveries up to 70%, and the results indicated that the treated effluent was within regulatory discharge standards. In addition, a hybrid process consisting of nanofiltration, reverse osmosis, and precipitation have been used to treat uranium effluents (72). The process removed both soluble and suspended uranium species; it was found that 95% uranium recovery was possible, and the treated effluent met environmental standards. The FT30 membranes gave uranium rejections of >99%. Cellulose acetate membranes have been shown to effectively remove 99% of uranium from effluents containing uranium nitrate when the uranium was complexed with ethylenediaminetetraacetato (edta) (73). Prabhakar and co-workers (74) showed that RO can be used to treat contaminated effluent from a uranium metal plant and 95% by volume of the treated effluent was within discharge limits. Arnal and co-workers (75,76) provide an in-depth discussion of the treatment of ^{137}Cs waste by RO. Their work follows the entire design process, from the preliminary studies examining the effects of radiation on membrane transport properties to the actual field application. A recent evaluation of membrane processes for nuclear waste treatment has been presented by Zakrzewska-Trznadel and co-workers (77).

6.4. Leachates. The treatment of landfill leachates serves two purposes. It facilitates the production of a water stream that can be discharged while concentrating the hazardous material and reducing its volume. Several studies have been conducted on the treatment of landfill leachates with RO processes. RO has been shown to be effective (high rejection at high recovery) in the removal of total organic carbon (TOC), total dissolved solids (TDS), chemical oxygen demand (cod), ammonia, heavy metals, and alkalinity from different types of leachates (3,111,112). In some cases, flux decline has been reported, however, proper pretreatment and membrane cleaning can alleviate this problem. In an early study, RO membranes were used to remove >91% of TOC from sanitary landfill leachate (111). In one case, RO treatment of landfill leachate resulted in removals of 94.5% alkalinity, 97% COD, 97% total solids, 92.1% volatile solids, and 96.6% ammonia (113). Bhattacharyya and Kothari (114) used FT30 membranes to treat soil-wash leachates containing heavy metals and organic contaminants so that the treated water could be recycled back to the soil-washing step. The TOC rejections as high as 80–85% and heavy metal (Pb, Zn, Ni, Cu) rejections of 94% to 98% were found. However, water flux decreases of up to 33% were noted. The effects of addition of edta or surfactant and feed preozonation were also investigated; feed preozonation substantially improved membrane water flux. Specific organic rejections included >98% for pentachlorophenol and 2,4-dinitrophenol, >97% for ethylbenzene, >81% for xylene, and >90% for chloroaniline. Lepore and Ahlert (115) reported the treatment of landfill leachates containing organic acids; they found good separations of volatile fatty acids, and TDS was removed sufficiently to allow discharge of the product water. Rautenbach and Mellis (78) reported that a commercial leachate treatment site in Germany was operational for >10,000 h without membrane replacement. Linde and co-workers (79) conducted tests on leachates from sites where the waste was segregated. Waste containing a large amount of ash was originally found to be unsuitable for treatment by RO. Recently, the problem of landfill leachate from incinerated waste has been addressed in Japan (116). Disk-tube RO has been used to remove the high levels of dioxins found to build up in leachates from incinerated waste. The concentrated dioxins are then efficiently destroyed by incineration. The total removal is > 99.9%.

Note that the complex chemical composition of landfill leachate often requires a combination of processes for effective treatment, typically involving membrane treatment as the means of water recovery (117). For example, adsorption and NF have been combined for the treatment of landfill leachate (118). The powdered adsorbent is added to the NF feed stream as a means of antifouling treatment. The adsorbent can then be recovered from the concentrate. The process has shown larger water recoveries, requiring lower operating pressures and costs than RO treatment.

6.5. Drinking Water. The ability of RO membranes to remove both inorganic and organic compounds has made them attractive for the treatment of contaminated drinking water supplies (80). Reverse osmosis processes can simultaneously remove hardness, various inorganics, such as bromate and bromide ions (81), color (82), many kinds of bacteria and viruses, and organic contaminants, such as agricultural chemicals and trihalomethane precursors. Eisenberg and Middlebrooks (83) reviewed RO treatment of drinking water sources, and they indicated RO could successfully remove a wide variety of contaminants. Membrane processes are also finding applications for the removal of natural organic matter (NOM) and disinfection by-products (DBPs). An excellent overview of selected processes (adsorption, coagulation, RO, NF, etc) for removing NOM and DBPs has been reported by Jacangelo and co-workers (84). Membrane processes showed the potential to achieve the highest removal of NOM and DBP precursors, but for surface water applications high pretreatment would be required to minimize fouling. A significant impact of RO and NF on the production of drinking water has been in the area of heavy-metal removal. Specifically, the need for the removal of toxic metals (ie, Pb, Zn, Ni, Ar) from various types of water supplies has received significant attention in the literature (85–89).

6.6. Municipal Wastewater. The application of RO membranes to the treatment of municipal wastewater has also had some success. Reverse osmosis can remove dissolved solids that cannot be removed by biological or other conventional municipal treatment processes. In addition, RO membranes can also lower organics, color, and nitrate levels. However, extensive pretreatment and periodic cleaning are usually needed to maintain acceptable membrane water fluxes. Early studies showed that high removals of TDS and moderate removals of organics could be achieved. Tsuge and Mori (90) showed that tubular membranes (with a substantial pretreatment system) could remove both inorganics and organics from municipal secondary effluent and produce water meeting drinking water standards.

The Water Factory 21 site in Orange County, Calif. is a large-scale municipal wastewater treatment site that has been studied in detail (91,92). The feed to the plant consisted of secondary effluent, and the process was composed of a variety of treatment systems, including RO membranes (several different types) with a 5-MGD capacity. The process reduced TDS and organics to levels that allowed the effluent to be injected into groundwater aquifers used for water supplies. Suzuki and Minami (93) reported studies on use of several RO membranes to treat secondary effluent containing various salts and dissolved organic materials. The TDS rejections of up to 99% and TOC rejections as high as 90% were found possible, and fecal coliform group rejections were >99.9%. Losses in water flux over time were noted, but could be partially restored by periodic cleaning. Recent efforts to combat the problems associated with treatment of municipal wastewater have led to the use of MF/UF pretreatment steps (3,94). Results from the use of such measures in Orange County have shown up to a 20% increases in water flux with a 40% reduction in total cost (95). Perhaps the greatest indicator of the impact of such pretreatment is the decrease in the frequency of cleaning cycles, from 4–6 weeks to 8–12 months (54).

6.7. Desalination. Desalination of seawater and brackish water has been and still is the primary use of RO. Driven by a need for potable water in areas of the world where there is a shortage of natural water, this industry has developed over the past few decades. Desalination involves the reduction of the TDS concentration to less than 200 mg/L. The RO offers several advantages over other desalination processes such as distillation, evaporation and electrodialysis. The primary advantage of RO over the traditionally used method of distillation is the energy savings that is afforded by the lack of a phase change in RO. However, the cost associated with RO can become unreasonable if care is not taken in the design and operation of a plant. For this reason, much attention has been given to process optimization in the literature (54–56). Since fouling presents one of the biggest financial burdens, many studies have focused on the development of more appropriate pretreatment schemes, as will be discussed below. In addition, more efficient energy use (lower cost) from the hybridization of RO with power production has been examined (54,57–60). Other improvements have come through the development of high performance membrane (12,56).

The RO processes for desalination were first applied to brackish water because brackish water has a lower TDS concentration. Brackish water has $<$ 10,000 mg/L TDS, while seawater contains $>$30,000 mg/L TDS. This difference in TDS concentration translates into a substantial difference in osmotic pressure and thus the required operating pressure to achieve the separation. The need to process feed streams containing larger amounts of dissolved solids led to the development of RO membranes capable of operating at higher pressures. There are currently desalination plants around the world that process both brackish water and seawater.

Most desalination plants use similar pretreatment and posttreatment methods in the desalting process. A block diagram illustrating the general procedure is located in Fig. 8**a**. The feed water is passed through multimedia, sand and cartridge filters to remove particulates and suspended solids. The feed water is typically treated with chlorine to kill any microorganisms in the water, followed by coagulation and filtration to remove the dead cells. For most commercially available membranes, dechlorination (with sodium bisulfite) before entering the membrane module is necessary to prevent membrane damage. Chelating agents and acid are injected into the feed water to prevent precipitation and scaling on the membrane surface. Permeate posttreatment usually consists of the addition of lime to increase the pH along with chlorine to prevent biological growth. In seawater desalination, the concentrated brine is usually returned to the sea. For brackish and well water desalination the brine must be disposed. An alternative pretreatment scheme, involving MF–UF–NF treatment is shown in Fig. 8**b** for comparison. The advantages of this scheme will be discussed below.

Currently, the largest desalination plant in the world is a brackish water plant in Yuma, Ariz. with a capacity of 275,000 m^3/day (61). The TDS concentration of the intake water is 3100 mg/L, producing product water with 200 mg/L TDS. Spiral wound cellulose acetate membranes perform the separation. As mentioned above, seawater desalination requires a much higher pressure to achieve a given separation than brackish water. The largest seawater desalination plant in the world operates in Jeddah, Saudi Arabia. It has a capacity of 56,800 m^3/day, and the TDS content of the seawater is $\sim$44,000 mg/L (62). Pretreatment modules for this plant include chlorine treatment, a dual media filter and a cartridge filter.

As mentioned, some desalination plants have combined the distillation process with RO to produce both power and water. Multistage flash (MSF) processes are used to produce both power and distilled water. Awerbuch and co-workers (60) reported on the combination of RO and MSF and the advantages of such a combination. Distillation processes typically reduce the TDS concentration to levels well below the required specifications. Since the product water from the two processes will be combined, the RO process can produce water at higher TDS concentrations while still meeting the potable water specifications. In addition, the power that is produced from the MSF process can be used in the RO process, cutting energy costs.

6.8. Ultrapure Water. Reverse osmosis has been used to produce ultrapure water for a variety of applications. The electronics industry require extremely pure water for the manufacture of semiconductors and other electronic components (96–98). For example, sodium should be present in no greater concentration than 1 part per billion (ppb) and there can be no >1 microorganism/mL. The RO can remove the low molecular weight organics that would pass through an ultrafiltration membrane. However, RO by itself cannot produce water of this purity. Rather, RO is merely one step in a hybrid of processes designed to achieve this level of purity. Ikeda and co-workers (99) reported the development of new membrane modules for ultrapure water production processes. These membranes showed very high rejections of TOC and inorganic ions at low concentrations. Okazaki and co-workers (100) reported on the use of an MF/RO treatment scheme at a Sony production plant in Singapore that allows for 40% of the processing water needs to be obtained from process waste streams.

The RO is also used to produce ultrapure water for many different uses in the laboratory (101) as well as in the medical and pharmaceutical industries (102). Once again, depending on the particular application, extremely pure water may be required in these industries. As with the electronics industry, the purity is achieved with a combination of processes. The order in which the various steps take place will vary from case to case.

6.9. Food and Beverage Processing. In certain processes, it is not the purified water, but rather the retentate that is the desired product. Often these applications involve the recovery of substances that are sensitive to changes in key process variables, such as temperature or pH. A common area illustrating this type of process is the production of concentrated fruit juices. Concentrated fruit juices are traditionally prepared using multistage vacuum evaporation. This process has many drawbacks, mainly high energy-consumption rates and loss of flavor/aroma molecules at the temperature/pressure required for evaporation (103). The use of RO presents an attractive alternative because of the ability to concentrate at low temperature. This also means that energy costs will be much less for RO when compared to evaporation. The one drawback is the inability of RO to feasibly concentrate the fruit juices to the desired level because of the large osmotic pressure gradient created at these levels. Research has been ongoing for 30 years to try and overcome this problem. Jiao and co-workers (103) presented an excellent review of advances in membrane technology in this field.

7. Nanofiltration

Nanofiltration (or loose RO) membranes have been investigated for a variety of separation processes, most often involving rejection of ionizable species. These membranes typically have much higher water fluxes at low pressures compared to traditional RO membranes. Nanofiltration membranes are usually charged (carboxylic groups, sulfonic groups, etc), and, as a result, ion repulsion (Donnan exclusion) is the major factor in determining rejection of charged species. For this type of separation, ion rejection increases with increasing valency ($SO_4{}^{2-} > Cl^-$). Rejection of noncharged species is solely based on size exclusion and governed by the pore size of the membrane (27). Another characteristic of charged membranes is the tendency to foul in the presence of components of opposite charge to that of the membrane (119). These membranes usually have good rejections of organic compounds with molecular weights >200–500 (120,121). Nanofiltration provides the possibility of selective separation of certain organics from concentrated monovalent salt solutions (eg, NaCl). An exhaustive review of NF literature has been given by Hilal and co-workers (27). They provide excellent discussions on NF membrane characterization, modeling and performance, and a wide range of NF applications. A brief overview of some of these concepts follows.

Although many types of membranes ranging from dense asymmetric structures to self-assembled thin films are available, the most important NF membranes are composite membranes made by interfacial polymerization. Typical polymers used include aromatic polypiperazine, polyamide, and cellulose acetate. Data concerning the permeability and SO_4^{2-} rejection for representative commercial NF membranes is included in Fig. 9.

A large effort has been put forth for the synthesis of new materials to allow for more specialized NF applications. For example, some attention has been given to the development and use of inorganic NF films because of their ability to operate in harsher environmental conditions, including extreme pH (low or high), non-aqueous solvent phase, and short-term exposure to high doses of gamma radiation (122). The films are often made from funtionalized alumina or silica. A promising new type of organic NF membrane based on layer-by-layer self-assembly of oppositely charged polyelectrolytes has been reported in the literature (123–127). Jin and co-workers (124) were able to get a 93.5% NaCl rejection at 40 bar using self-assembled layers of polyvinylamine and polyvinylsulfate on PAN/PET supports. Recently, characterization of NF films has involved intense AFM probing that can provide data describing the diameter, density, and size distribution of the membrane pores (27). This data is needed to develop models that can accurately describe and predict the behavior of NF systems. Traditionally, this data had to be obtained through rigorous rejection studies. In addition to pore characterization, AFM has also been used to gain some insight into the role of surface morphology (roughness) in separation mechanisms (27).

Modeling the NF Process. As mentioned above, NF membranes separate species using both charge and size exclusion. Therefore, models to describe this process must include both steric and electrostatic effects on mass transport. The traditional starting point is the extended Nernst-Plank equation, which describes the electrostatic effects on the transport of charged species. This equation can be combined with appropriate terms describing steric effects to derive a model that can accurately predict the rejection of all solutes through NF membranes (27). Some of the more prominent of these models are the electrostatic and steric-hindrance model (ES) and Donnan-steric-pore model (DSPM), which often show good agreement with experimental results (27). Other approaches to modeling based on the Spiegler-Kedem model (or its modified forms) have been presented (27). These models are often limited to specific cases in their application. Recent efforts in modeling transport through NF films have focused on the nonequilibrium thermodynamic approach and use the Maxwell-Stefan equations as their starting point (128). This approach is beneficial in that can lead to models that accurately describe system performance, without the need for an adjustable parameter.

Applications. Nanofiltration has been used in several commercial applications, including demineralization, organic removal, heavy metal removal, color removal, pharmaceutical recovery, treatment of pharmaceutical wastewater, production of concentrated fruit juices, and RO pretreatment (27,85,129–135). Bindoff and co-workers (136) reported the use of NF membranes to remove color-causing compounds from effluent containing lignins and high salt concentrations in a wood pulping process. Color removals were >98% at water recoveries up to 95% while the inorganics were poorly rejected, allowing the use of low operating pressures. Ikeda and co-workers (137) indicated NF could give high separations of color-causing compounds, such as lignin sulfonates in paper pulping wastewaters. Afonso and co-workers (138) found NF removal (>95%) of chlorinated organic compounds from alkaline pulp and paper bleaching effluents with high water fluxes. Simpson and co-workers (139) reported the use of NF membranes to remove hardness and organics in textile mill effluents. Perry and Linder (140) discussed the recovery of low molecular weight dyes from high salt concentration effluent. Ikeda and co-workers (137) and Cadotte and co-workers (121) reported the use of NF membranes in the treatment of food processing wastewaters. Some specific uses included the desalting of whey and the reduction of high BOD and nitrate levels in potato processing waters (141).

The NF processes are also finding wide applications in drinking water production by removing natural organics and hardness from raw water, which cause trihalomethane (THM) formation during coagulation (129). The NF membranes have been used to remove organic matter from highly colored groundwater (142), as well as from river water (143). Rautenbach and Mellis (144) used NF in a hybrid process with biological treatment and chemical oxidation to treat leachate from a dumpsite. They observed increases of 9–17% in the elimination rate as compared to a process without nanofiltration. Recently, Nghiem and co-workers (130) reported the potential use of NF membranes to remove natural hormones from drinking water. These hormones are released into the environment by humans and animals and present a major health risk as an endocrine disrupting chemcial.

The removal of toxic metals (Cd, Ar, Ni, Ur, Pb, Hg) and organics has received significant attention in the literature. Bhattacharyya and co-workers (145) used NF40 (Dow/FilmTec) membranes to selectively separate mixtures of cadmium and nickel. Williams and co-workers (146) and Bhattacharyya and Williams (147) examined NF40 membranes with and without pretreatment by feed preozonation to study removal of various chlorophenols and chloroethanes. The TOC rejections up to 90% were possible with ozonation pretreatment. Chu and co-workers (72) detailed the use of NF in a process for treating uranium wastewater; NF40 uranium rejections were 97–99.9%. Dyke and Bartels (148) discussed the use of NF membranes to replace activated carbon filters for the removal of organics from offshore produced water containing residual oils. The produced waters contained ~1000 mg/L soluble organics (mostly carboxylic acids) and high inorganic concentrations (~15,000 mg/L Na^+ and ~25,000 mg/L Cl^- as well as other dissolved ions). Organic rejections were suitable to meet discharge standards while inorganic rejections were low (<20%), allowing operation at low pressures.

The development of charged membranes with tuneable properties for metal removal has provided the opportunity for highly selective separations using materials with hydraulic properties (pore size and distribution, tortuosity) in the range of MF films. These materials utilize the pH-based structural response of charged macromolecules (polyelectrolytes) to alter the flow path and charge distrubution within a membrane pore. For example, Hollman and co-workers (149) attached poly-L-glutamic acid (PLGA) to the pores of cellulose mats for the separation of toxic metals. It is well known that PLGA will undergo a conformational change from a tight helix coil at low pH (<4) to a more random, dangling coil at moderate to high pH (>5.5). The advantage of this is that the effective pore radius for flow, r_c, and the charge distribution within the membrane pores can be “tuned” by adjusting the pH of the feed solution. As the PLGA uncoils into the pores, the pore radius for flow, defined as the difference in the unfunctionalized pore and twice the PLGA chain length, decreases. At the same time, the magnitude of the electrostatic field in the flow field increases. The impact of these responses can be adjusted to allow selective separation of ions based on size and charge. This concept is shown in Fig. 10.

A similar approach has been reported in the literature that uses polyelectrolyte gel-filled microporous membranes to provide a “tuneable” separation. A complete discussion of these systems has been given by Childs and Mika (150). This approach is an extension of supported liquid membranes. In this case, transport through the membrane will occur in the gel phase, which is anchored within the pores to prevent it from being washed out. For most NF-type applications, the gel phase is typically a highly hydrophilic polymer network that swells from solvent (water) uptake. This swelling will ultimately decide the rejection characteristics of the membrane. Swelling is mainly a function of the polyelectrolyte concentration and degree of cross-linking, as well as the pH of the feed. Since transport actually occurs through the water phase within the gel, the permeability of the film will depend largely on swelling, and to some extent the porosity and tortuosity of the support membrane. The impact of swelling on permeability is related to the formation of solvent-rich transport (draining) zones within the gel network. Although one would expect a more swollen gel to provide an enhanced permeability, experimental results have shown that the opposite is actually the case. As the polymer-solvent (gel) network collapses, the system becomes more heterogeneous in nature, resulting in an increase in “drain-zone” volume within the poor.

Separations in Non-aqueous Media. A relatively young, but expanding application of NF/RO is the treatment of waste streams and recovery of materials involving non-aqueous solvents (151–158). The use of NF membranes in non-aqueous medium holds strong potential for the food, refining and pharmaceutical industries because of the low energy costs involved with such membrane processes. Possible applications of this type are shown in Fig. 11. Full scale-applications involving solvent lube oil dewaxing (151,152) for refinery operations have been reported in the literature. ExxonMobil in conjunction with W. R. Grace Company have developed a membrane-based process where the membrane reduces the residence time for the solvent mixtures and thus allowing faster processing of the solvent. The membrane was typically operated at a low temperature of -10°C and a pressure of 41 bar with 20 wt% lube oil in the feed. The cold solvent was directly recovered from the permeate and recycled back into the process. The membrane used in this process was a developmental asymmetric polyimide-based membrane that can withstand the corrosive solvent blend (MEK and toluene) used in the application. The process has been scaled-up from the lab scale to the commercial scale by ExxonMobil in Beaumont, Texas and is called as the MAX-DEWAX process. Solvent resistant membranes are also very valuable for pharmaceutical product recovery and for the recycle of homogeneous, Rh or Pd based organometallic catalysts (153).

Separations involving non-aqueous media are often more complex than aqueous systems because of the potential impact of the solvent on the membrane (swelling, degradation, etc). In addition, the solutes, solvent, and membrane often all possess similar chemical structures (hydrophobic backbones with possible hydrophilic functionalities) that can lead to poor separations depending on the magnitude of the solute–solvent, solute–membrane, and solvent–membrane interactions. It is possible to even achieve negative solute rejections if the solute strongly adsorbs to the membrane surface, resulting in increased membrane flux.

Solvent-resistant membranes are typically synthesized from aromatic polyamide-, polyimide-, or silicone-based materials. In the same manner that the recovery fraction of water is crucial to aqueous separation systems, the solvent recovery fraction in non-aqueous systems must also be considered. An improper choice when considering the type of membrane polymer can result in a significant reduction of solvent flux and poor recovery fractions. For example, Bhanushali and co-workers (155,156) studied the transport of typical solvents through selected commercial membranes. They found that pure methanol flux through a Desal HL (GE Osmonics) membrane is ~25 times greater than the flux of ethyl acetate. When the flux measurements are made using an MPF 60 (Koch) membrane, the ethyl acetate flux is about three times greater. This is expected if one considers that the Desal HL membrane is hydrophilic and the MPF 60 is hydrophobic. Thus membranes and membrane processes offer an excellent avenue in downstream processing with their versatility and low energy requirements. For solvent-based membrane applications, in addition to membrane stability module packaging consideration is also critical.

8. Organic Separation From Aqueous Streams

The separation of organics from aqueous streams, even at dilute concentrations, can be quite complex. In addition to size exclusion, the interactions of the solute with the membrane polymer will have a tremendous impact on the observed rejection and water flux (159). Original studies focused on the rejection behavior of common RO films. Recently, NF and ultralow pressure (ULP) RO have been studied in the literature for organic separations because of the lower costs associated with these processes. Bellona and co-workers (159) provided an excellent review of literature addressing the factors affecting organic solute rejection by NF/RO membranes. Their work examines both solute (molecular weight and size, acid dissociation constant, hydrophobicity–hydrophilicity, diffusion coefficient) and membrane (molecular weight cut-off, pore size, surface charge, hydrophobicity–hydrophilicity, surface morphology) parameters known to influence organic solute behavior. A discussion of some of the key aspects of organic separations follows.

8.1. Organic Rejections. Extensive work has been performed examining the separation of organics using pressure-driven processes. Some of the earlier work by Sourirajan (160) and Sourirajan and Matsuura (10) detailed the separation and flux data of cellulose acetate membranes for a large number of organic compounds. They found that organic separation varied widely (from <0 to 100%) depending on the characteristics of the organic (polarity, size, charge, etc) and operating conditions (such as feed pH, operating pressure, etc).

As membrane materials have advanced, the data available in the literature has grown to include a variety of RO and NF membranes. Košutić and Kunst (161) studied the rejection of petrochecmicals and pesticides using RO, ULPRO, and NF commercial membranes. Agenson and co-workers (162) studied the rejection of a variety of semivolatile (SVOC) and volatile (VOC) organic compounds by NF membranes with salt rejections ranging from low (loose) to high (dense). Schutte (163) studied the separation of alcohols and phenols using both aromatic polyamide TFC and asymmetric CA RO membranes. Selected rejection data for representative membranes is shown in Table 3. Sodium chloride rejections, where available, have been reported as a rough indicator of how dense the membrane is. For the case of alcohols and phenols, the reported rejections are for the non-ionized form ($\mathrm{pH} < \mathrm{p}K_a$). Upon examination of the data, key trends in organic separation become apparent.

For many cases, rejection tends to be a strong function of molecular size. Larger molecules cannot diffuse through the membrane pores and will be rejected. To quantify this, attempts have been made to correlate organic rejection with molecular weight (159,161–164). Because of this, membranes are typically classified based on their molecular weight cut-off. While this does give some measure of a molecule's size, it does not take into account the geometry of the molecule. Therefore, Agenson and co-workers (162) proposed the use of molecular length and width parameters to better predict rejection. These parameters account for the volume of a molecule (branched, linear, etc). Molecules with larger volumes will have higher rejections. Perhaps the most common parameter used to describe solutes is the Stokes radius, which is a strong indication of the diffusivity that solute will have within the membrane. A membrane will better reject solutes with smaller diffusivity values (164).

8.2. The Water–Membrane Interface. In cases where rejections deviate from size-related trends, the interaction of the organic at the water–membrane interface must be considered (161). For rejection to occur, there must be preferential sorption of water over the organic by the membrane. For uncharged organics, this will be affected by water solubility (hydrophilicity), hydrogen bonding, and molecular polarity (159,161–164). For example, 2-butanone is known to have a significant dipole moment, and therefore has the flexibility in its bonds to countersteric effects within a dense PA TFC RO film, resulting in a lower rejection of only 54% (161). Hydrophilicity (or hydrophobicity) is often discussed in terms of an octanol–water partition coefficient. Organics with larger values of

K_{OW} are more hydrophobic. Since membranes are typically hydrophobic, hydrophobic organics can become strongly adsorbed to the membrane surface. Some researchers suggest that the observed rejection is really a measure of this adsorption (159). This theory is supported by the reported decline in rejection for strongly interacting organics after the solubility limit within the membrane is reached (159). Although it does provide some insight into rejection, attempts to correlate rejection with K_{OW} have not proven insightful.

Perhaps of more importance is hydrogen bonding and polarity. At the molecular level, solute interactions with the membrane are based on the interaction of electrons. For favorable interactions, the organic must have a greater affinity for electrons (basicity) than the membrane, which is based on the type of substituent groups present (162). Organics containing alcohols, aldehydes, ketones, and chlorinated constituents have shown strong interactions with membrane surfaces. This effect is normally quantified using the Taft number (159,162). As the Taft number decreases, electron attraction decreases, which results in less favorable interactions with the membrane surface versus water and higher rejections (162). In addition to unwanted organic transport, the adsorption of organics to membrane surfaces has been shown to dramatically decrease water flux by blocking membrane pores (159). This has prompted several manufacturers to develop membranes with charged surfaces (decreased hydrophobicity) to hinder organic adsorption (159).

For the case of charged systems (solute and/or membrane), electrostatic effects must be considered. For ionizable organics, rejection behavior changes significantly when the pH of the feed is increased above the corresponding pK_a because Donnan exclusion will dominate the rejection mechanism. Ozaki and Li (164) showed that the rejection of acetic acid by a negatively charged ULPRO membrane was increased from 35 to 99.7% when the pH was raised $>$ p$K_a = 4.7$. Similarly, the same behavior can be expected for other ionizable species because of the strong electrostatic repulsion that can occur when the charged molecule comes close to the membrane surface. The rejection of phenols by the ULPRO membrane was even found to increase linearly with increasing pK_a. Exceptions to this occurred for molecules, such as aniline, which carried a positive charge upon dissociation. These molecules experienced a decrease in rejection as the pH is increased because of stronger adsorption to the negatively charged membrane surface. Since most membranes contain surface charge, the pK_a and operating pH become crucial for the separation of charged organics.

Solute–membrane interactions have been both measured and calculated. Sourirajan and Matsuura (10), Jiang and co-workers (165), and Gao and Bao (166) used liquid chromatography with the membrane polymer as the column packing in order to directly measure inorganic and organic solute–membrane interfacial parameters, such as equilibrium distribution coefficient, Gibbs free energy, and surface excess for a large number of different polymers. Sourirajan and Matsuura (10), Bhattacharyya and co-workers (47), and Mehdizadeh and Dickson (44) also used the SFPF model in order to calculate solute–membrane interaction forces (Coulombic or van der Waals). Jiang and Jiayan (167) characterized interactions of organic solutes with poly(benzimmidazole) membranes using quantum chemistry calculations, liquid chromatography, and infrared (ir) spectroscopy.

8.3. Modeling Organic Separations. The vast amount of data available has led to the development of several models for organic separation. Models describing organic separations by RO membranes generally fall into one of four groups based on the starting theory: (*1*) solution–diffusion, (*2*) solvophobic, (*3*) solubility parameter–charge effects, and (*4*) irreversible thermodynamics (159). For solution–diffusion models, the traditional SD equations are modified by incorporating an organic sorption term (168) or by solving the general diffusion-convection equations with organic adsorption terms (53). A modified solution diffusion (MSD) model can easily be obtained by assuming that the sum of organic and water concentrations is constant (total concentration in membrane, $C_{\mathrm{tm}} = C_{\mathrm{m}} + C_{\mathrm{wm}}$), and representing $C_{\mathrm{m}}/C_{\mathrm{tm}}$ by a Langmuir adsorption term. The modified SD equations for water and solute flux will be

$$J_{\mathrm{w}} = \left[\frac{1}{1 + b_0 C_{\mathrm{F}}}\right] A^{*}(\Delta P - \Delta\pi) \tag{9}$$

$$J_{\mathrm{s}} = B^{*}\left[\frac{b_0 C_{\mathrm{F}}}{1 + b_0 C_{\mathrm{F}}} - \frac{b_0 C_{\mathrm{P}}}{1 + b_0 C_{\mathrm{P}}}\right] \tag{10}$$

The impact of organic interactions on both sorption and diffusion is accounted for through a modified water permeability parameter (A^*) and an organic–membrane interaction parameter (b_0). As expected, flux decreases significantly with increasing b_0. This type of model has one disadvantage in that it is not applicable for the emerging porous ULPRO and NF membranes. For these films, other theories are necessary that account for pore flow. In some cases, convection terms have been added to the SD model with some success (159).

Solvophobic theory uses the net free energy change associated with the adsorption of a molecule based on its total cavity surface area (TSA) to account for rejection behavior (163). In addition, the influence of charge interaction and hydrodynamic shape is incorporated. For derivations of such models, an appropriate shape factor must be defined. This is often the source of variation amongst the different models. The TSA values must typically be calculated using rigorous computational procedures since their availability in the literature is scarce. To get around this, Schutte (163) proposed a correlation of TSA with molecular weight for separations involving nonpolar membranes. The predicted rejections using TSA values obtained from the correlation were lower than experimental values because molecular weight does not account for geometric effects like branching.

Solubility parameters, such as the Flory–Huggins interaction parameters, have been incorporated into several types of transport equations developed for inorganic separation. These parameters can be used to predict the ability of a solute to partition into the membrane. For systems involving charged species, the transport equations are based on the extended Nernst-Planck equation. Use of these models will obviously require knowledge of the solubility parameters, as well as the charge characteristics for a given system. Often times, numerical solutions are difficult and must be obtained using computational mathematics.

The derivation of models using irreversible thermodynamics has also received attention in the literature (159,169). As previously mentioned, this type of model examines the various driving forces occurring within a transport system through the use of phenomenological coefficients. Solute–membrane interactions can be incorporated into these equations, allowing their application to organic separations.

For ternary systems, the influence of the second organic must be considered. Often times, this is accomplished through modifications of the Kimura-Sourirajan analysis (SD model). Weißbrodt and co-workers (169) used this approach to model the transport of a target organic from ternary systems. This is the first attempt to take into account physiochemical effects during the competitive transport of organics. Their method differs from Kimura-Sourirajan analysis because a dimensionless separation factor for the target organic is used in place of the traditional separation factor proposed for the SD model. This factor is based on molar flow, dipole moment (molecular shape), molar mass, and molecular interactions (obtained from the Stokes equation). The use of the Stokes equation allows for temperature effects to be included since diffusivity and water viscosity are functions of temperature. The new factor was used to empirically fit experimental rejection data for different types of compounds (alcohols, ketones, etc) using three adjustable parameters. Predicted rejections for some species showed as little as 0.2% error with experimental results.

9. Fouling

One of the primary concerns in any membrane process is the irreversible fouling of the membrane surface, which can lead to product flux decline as well as possible changes in rejection and selectivity. Fouling is a broad term that refers to the deposition or association of solutes on the membrane surface or within the membrane pores, which consequently leads to a decrease in the membrane performance. The cause of fouling can generally be traced to constituents in the membrane feed stream. Several general categories of foulants found in process streams can be identified in relation to RO and NF processes: biological fouling, colloids, scaling, organics, metal oxides, and suspended solids. Depending on the particular application, one or several of these categories may become a factor in the RO process. For example, the desalination of seawater may have problems with colloids, suspended solids, biological fouling and scaling. Wastewater reclamation, on the other hand, suffers from fouling by dissolved organics and biological slime. Fouling must be taken into consideration when considering the use of RO on an industrial level.

The manner in which the foulants decrease the membrane flux varies depending on the particular foulant and type of membrane. For example, Hoek and Elimelech (170) studied colloidal fouling of commercial TFC RO and NF membranes and determined cake-enhanced concentration polarization is the dominant fouling mechanism for salt-rejecting membranes. The build up of rejected ions within the cake layer causes a sharp increase in the feed side osmotic pressure, which leads to the decline in performance. On the other hand, Zhu and Elimelech (171) compared fouling tendencies of cellulose acetate and composite polyamide RO membranes and determined that hydraulic drag played a larger role than chemical effects. They also concluded that surface morphology, mainly increased roughness, plays a key role in the onset of fouling based on the shorter fouling times for the much rougher composite films.

Gel layers can be formed at the surface from a variety of constituents that do not enter the membrane but accumulate at the surface. In the presence of inorganic salts at high water recovery, solubility limits can be exceeded causing the formation of a scale on the membrane surface. Various microorganisms can attach and grow on the membrane and thus create a biological slime. Other components that can form gel layers are humic acids, proteinaceous material, and other large molecules. In the presence of fine colloids or suspended solids, the membrane may also become plugged.

The success of a reverse osmosis process hinges directly on the pretreatment of the feed stream. If typical process streams were contacted with the membranes without pretreatment to remove partially some of the constituents listed above, membrane life and performance would be unacceptable. Unfortunately, there is no single pretreatment step for all types of foulants. Depending on the number, nature, and concentration of the foulants in the feed stream, a logical pretreatment train must be developed for the success of the RO plant. Pretreatment methods range from pH control to adsorption to filtration, depending on the chemistry of the particular foulant. Table 4 lists some of the common pretreatment methods for each type of foulant.

Biological components form slimes on the membrane surface that cause a reduction in the membrane flux as well as membrane degradation (172,173,175,176). Steps such as chlorination (0.5 mg/L) are generally taken to kill the biological constituents before the feed enters the membrane module. Chlorine, unfortunately, can cause damage to most RO membranes. Typical cellulose acetate membranes can withstand chlorine concentrations of 0.3–1.0 mg/L, while polyamide membranes can withstand <0.05 mg/L. Therefore, any pretreatment that uses chlorine must have an additional step for chlorine removal, the most common of which is the use of sodium bisulfite. Too much residual chlorine after the removal step can lead to membrane damage that, in turn, usually leads to an increase in flux with a dramatic decrease in rejection. If, however, all of the chlorine is removed while a few bacteria remain, the bacteria can continue to grow. For this reason, it is desirable to have a chlorine resistant membrane to prevent biological growth by allowing a low concentration of chlorine to be present in the RO module. There has been considerable research on chlorine resistant RO membranes (177–181). Gaeta and co-workers (177) used a poly(*trans*-2,5-dimethyl)piperazinthiofurazanamide in the presence of low concentrations of chlorine and report a membrane life of 3 years when exposed 3 mg/L Cl_2. Nita and co-workers (178) developed a new copolyamide hollow fiber membrane for use in desalination and have shown it to be resistant to 0.5 mg/L chlorine.

As mentioned above, inorganic salts can precipitate on the membrane surface if the solubility limit of the salt is exceeded, which may occur with increased water recovery. Depending on the types of salts present in the feed stream, different steps can be taken to prevent scaling. For waters containing bicarbonates and calcium, $CaCO_3$ presents a potential scaling problem. Treatment of the water with acid converts the bicarbonate to carbon dioxide and eliminates the scaling problem (182). Calcium and magnesium can be removed by precipitation with lime and subsequent removal. Chelating agents such as EDTA and polyphosphates are also frequently used to prevent precipitation.

Metal oxides found in RO feed streams typically originate from corroded pipes found in the RO process. These metal oxides can deposit on the membrane surface and decrease the membrane flux. This type of fouling can be prevented if the proper materials of construction are used in the piping system to prevent corrosion.

Suspended solids can accumulate at the membrane surface creating an additional resistance to flow through the membrane as well as possible feed channel (eg, for spiral wound module) plugging and subsequently a decrease in flux. Prevention of this type of fouling lies in the removal of the suspended solids prior to the RO unit, which can be done using filters and screens.

Colloidal materials present in surface waters can plug RO membranes and cause a decrease in permeate flux. They can be removed in one of several ways. The most common method involves the addition of coagulant, such as alum to the water to form aggregates of the colloid, which can then be filtered similarly to suspended solids.

Proteinaceous material is often found in process streams in the textiles and food industries, where RO is used to clean wastewaters. The effect of proteinaceous material on membrane performance has been investigated extensively in ultrafiltration and microfiltration, however very little work has been done in the RO area. Because the use of RO is growing in the area of wastewater treatment, there is a significant interest in determining the cause of proteinaceous fouling and methods of prevention. The size of protein molecules prevents them from entering the membrane matrix. Instead, they accumulate at the surface forming a gel layer and creating an additional resistance to flow through the membrane. Parallels can be drawn between RO and the other membrane processes mentioned. Depending on the isoelectric point of the protein in question, the pH of the feed stream and the charge of the membrane, electrostatic interactions may cause association of proteins on the membrane. In MF and UF, surface modifications to impart hydrophilicity on the surface have been one method of prevention of fouling by proteinaceous material.

Although each is effective in its own way for removing foulants, the traditional pretreament methods discussed do have their drawbacks. In addition to the cost of chemical additives and adsorbants, sometimes the chemicals themselves can cause a degradation of process equipment (27,174). Also, the economics of conventional pretreatment do not allow for complete elimination of all foulants, requiring cleaning cycles to be incorporated into unit operation (174). Therefore, researchers have studied the feasibility of eliminating these cumbersome steps by switching to pretreatment based solely on pressure-driven filtration, including MF, UF, and NF. Recently, Hilal and co-workers (27) reviewed the use of membrane filtration steps, including MF, UF, and NF for pretreatment of RO feeds. The advantage of MF is that it can remove suspended solids and silt. With UF pretreatment, large and small bacteria, macromolecules, and colloids are also removed. The use of NF as a pretreatment step is starting to gain attention for its ability to remove ionic species (including boron) and lower TDS, helping to prevent fouling in the RO module. An equally important gain in RO performance also results from the use of NF. The reduced TDS and ionic levels mean smaller operating pressures are required and larger recoveries can be obtained. The benefit of larger recoveries will be discussed below. The important thing is that a reduction is achieved in the cost of water produced. Redondo (183) studied the use of MF/UF as pretreatment for an RO process producing 2000 m^3/day and found that use of such steps would require an operating cost of \$0.35/m^3 of permeate produced. This is a 30% reduction in pretreatment operating cost when compared to the \$0.49/m^3 of permeate associated with conventional pretreatment.

Methods for cleaning membranes have been developed over the years (184–186). Cleaning methods (Table 5) can be divided into two classes: chemical and physical. Physical cleaning can only be performed on flat plate (scrubbing) or tubular membranes (sponge balls). For the hollow fiber and spiral wound modules, which offer the advantage of high surface area, physical cleaning is not an option. Chemical treatments must be used to remove the fouling layer in these types of modules. Common chemical cleaning agents for this purpose include alkalines, acids, metal chelating agents, surfactants, and enzymes, with typical commercial cleaners containing a mixture of these (187). For example, calcium scales can be removed by the use of citric acid. Once again, knowledge of the feed stream, and hence the foulants is of the utmost importance when cleaning membranes.

10. Design and Economic Considerations

There are several considerations that should be made to ensure a successful design of a reverse osmosis process. These considerations encompass the feed solution, the membrane module, and the use of other processes in the pre- and posttreatment steps. A good knowledge of the feed stream and its components is necessary to prevent membrane damage and product impurities. Once the feed stream is characterized and the process objective is defined, the design of the process can be initiated. A brief discussion of some general considerations along with some recent developments in the design of reverse osmosis follows.

Feed characterization (particularly for nondesalination applications) should be the first and foremost objective in the design of a reverse osmosis plant because it will determine the type and extent of pretreatment necessary. This involves the determination of the type and concentration of the main solutes and foulants in the stream, temperature, pH, osmotic pressure, etc. Since feed pretreatment generally adds to operating costs, this step should use the minimum technologies necessary to meet the process objective. Once feed quality after pretreatment has been established, the membrane module network can be specified.

Design of the membrane module network involves selection of the membrane material, module geometry (spiral wound, hollow fiber, etc), product flowrate and concentration, solvent recovery, operating pressure, and the minimum tolerable flux. Since module geometry and solvent recovery are normally chosen to minimize fouling, spiral wound modules are widely used because they offer both high surface area as well as a lower fouling potential. After these variables have been fixed, simulations are required to establish both the number of membrane modules required and the best configuration for operation.

The traditional simulation first determines the performance of an individual membrane module, which is then used to specify the configuration of the module network based on economic constraints. A model that governs transport through the membrane must be used to predict module performance. Several models describing membrane transport have already been discussed, ranging from the SD model to the irreversible thermodynamics model. Each model is limited by its assumptions, and therefore limited in its range of applicability. Simulations that make use of these models have been developed for several systems. Brouckaert and Buckley (188) used data obtained from a pilot plant in the treatment of cooling tower water by tubular reverse osmosis to simulate a full-scale plant. Their simulation uses the finely porous model for transport through the membrane. Malek and co-workers (189) used the SD model to simulate the transport of a saline solution through a Dupont B10 permeator. A finite element technique was used by Bhattacharyya and co-workers (51) to predict the concentration polarization in a parallel plate membrane module, which involves the solution of convection-diffusion equation, given a mass transfer model and boundary conditions. This model was used to determine the effect of the operating variables on the flux and rejection behavior of NaCl systems.

Since changes in the performance of any module within a network will affect all other modules downstream of it, the performance of the entire network must be evaluated simultaneously. After all process variables have been calculated, the costs associated with the process can be estimated. Ray (190) has reviewed the costs associated with RO processes. Capital costs will include equipment, land, installation, and utilities. The equipment costs will include the necessary components for pretreatment of the feed, storage of the product, pipes and pumps, and the RO module. Equipment costs range from \$400/(m^3/day) for brackish water plants to \$900/(m^3/day) for seawater plants. Operating costs include the usual costs for an industrial process: energy, labor, and chemicals. For any membrane process, there are additional operating costs due to membrane replacement. Membrane replacement costs range from \$0.05/m^3 for brackish water plants to \$0.10/m^3 for seawater plants. Energy consumption in reverse osmosis is usually the largest operating cost because of the high pressures that are required for seawater desalination plants. Energy costs have been reported from \$0.10/m^3 to \$0.40/m^3.

The optimal membrane module network can be found by minimizing the above costs. Since the entire design process can be tedious, much effort has gone into developing computational methods for this task. Niemi and Palosaari (191) integrated a model into a process simulation program to predict the stream matrix for a reverse osmosis process. The proper placement of RO modules so as to achieve the minimum waste at a minimum cost is essential. El-Halwagi (108) provides excellent details on how to create an optimal network of RO modules. Several commercial design software packages are also available that can aid in all aspects of design and operation of RO plants [WINFLOWS v1.2 (GE Osmonics), ROSA v5.4 (Dow Chemical), etc].

Designing successful NF systems is accomplished using the same techniques employed in RO design. Mohammad and co-workers (192) presented a detailed description of this approach for a typical NF system. As with RO, a suitable transport model must first be used to predict process performance. The most common model used for NF processes is the previously discussed DSPM model. Optimization is made possible by incorporating the transport results into an appropriate cost model. A typical cost model identified by Mohammad and co-workers (192) is the Verbene cost model, which accounts for both capital and operating cost associated with membrane processes. The economic impact of changes to process variables can be assessed in this manner, allowing for the selection of ideal operating parameters. One advantage of this method is that membrane properties can be incorporated into the cost to help with membrane selection. Using this approach, it is possible to determine the cost breakdown for a given NF system. For example, Van der Bruggen and co-workers (193), using a similar approach, found that an optimized NF system operating at 8 bar would have the following cost distribution: depreciation (32%, operation and quality control) 23%, energy usage (18%), chemical materials (16%), and maintenance (11%). Obviously the largest cost associated with membrane system is the actual equipment depreciation cost (membrane replacement), which illustrates the importance of proper equipment selection.

10.1. Advancements in RO and NF Technology. Ultimately, the ability to apply RO and NF technology to emerging separation demands requires the development of more sophisticated materials that can withstand the most extreme environmental conditions. The feasibility of using RO and NF will depend on improvements to existing processing capabilities. To accomplish this, research efforts have addressed three key areas: (*1*) fouling prevention, (*2*) process hybridization and water (solvent) recovery, and (*3*) enhanced separations. A discussion of some of the advances in these areas is presented.

Fouling. As the application of RO and NF technologies has become more widespread, the need for more extensive measures to prevent membrane fouling has presented many challenges to researchers. The efforts to minimize fouling in membrane processes can be grouped as follows: (*1*) feed pretreatment as dicussed earlier, (*2*) development of antifouling membrane materials, and (*3*) preventative maintenance (chemical cleaning/backwashing). The common goal of all three is to help minimize process cost by maximizing the operating cycle length for a given membrane.

The development of the Extended-DLVO theory describing particle interactions has provided the unique opportunity to address the problem of fouling on a molecular scale. For any foulant to deposit, a strong adhesive bond must be formed, resulting from the charge interactions of the foulant and membrane surface (194). Deposition of foulants will also depend on the flow of the feed solution over the membrane surface, since adhesive forces must be stronger than shearing forces. As the knowledge of how these interactions occur during membrane separations has grown, more attention has been given in the literature to the development of “antifouling” surfaces. The goal of this type of work is to develop membranes that provide a separation performance (flux and rejection) comparable to current commercial membranes while offering surfaces that are less favorable for adhesive bonding with foulants. Typically, this either involves producing much smoother membrane surfaces or chemically modifying surfaces to control either the charge distribution or contact angle (159,195,196).

All of these research efforts show tremendous promise in overcoming the problem of fouling in the future. However, they do not present much relief for existing membrane facilities. Therefore, preventative maintenance (cleaning and backwashing) is necessary to guarantee satisfactory process performance. Li and Elimelech (187) studied both the fouling of NF-270 membranes by NOM and its removal using model chemical cleaning agents. They first examined the impact of total ionic strength and divalent cations (Ca^{2+}) on NOM deposition and found that Ca^{2+} had the only significant effect. The chemical agents tested included deionized water, an alkaline solution, metal chelating agent, and anionic surfactant. In the absence of Ca^{2+}, the initial fluxes could be recovered using all of the cleaners. For cases where Ca^{2+} was present, only the metal chelating agent and anionic surfactant were effective. These results emphasize the importance of pretreatment on process performance. Obviously, softening for removal of Ca^{2+} would be desired for any process involving membranes susceptible to this type of fouling.

The key to any successful maintenance program is reliable monitoring and early diagnosis of the onset of fouling (197). The standard method for monitoring fouling in membrane processes is ASTM D-4516, which uses the monitoring and comparison of normalized flux data to detect fouling within the process. A performance curve (flux behavior for a given time period) supplied by the manufacturer is used to determine the onset of fouling. These curves are often based on the manufacturer's laboratory experiments that do not accurately simulate the specific operating conditions at a plant. So data must be collected over a long-time period for accuracy. Recently, Saad (197) has concluded that such a system is flawed because it is typically unable to reliably identify fouling until it is too late. Often fouling at the point of identification can be severe enough to cause irreversible loss in performance and damage to the membrane. Instead, he discusses the advantages of a real-time monitoring system that identifies fouling based on deviations of the normalized flux data from the performance curve for the same operating time. Increases in the magnitude of deviation indicate fouling in the system. Two case studies involving the use of real-time monitoring in place of the ASTM D-4516 method showed significant performance improvements, both in terms of operation time between cleaning cycles and recovery from fouling. An improvement like this is significant because it can lead not only to a reduction in operating cost for RO and NF, but for all membrane processes.

Hybrid Processes and Increased Water Recovery. For most wastewater applications, the use of a single type of technology (ie, RO, NF, adsorption, stripping) will not be adequate enough to achieve process goals involving the simultaneous recovery and reuse of multiple components. This fact has led to the use of various integrated (or hybrid) separation methods combining the benefits of each type of process to achieve highly selective separations. For example, the waste-streams generated in a dye plant often contain unused dye and dissolved salts. Recycling the dye and purified water back to the process can reduce operating costs. Allegre and co-workers (198) proposed an integrated membrane process for this purpose. A representation of their process is shown in Fig. 12. In this case, an NF membrane is used to separate and concentrate the dye. The permeate is fed to an RO unit to recover high quality water to add back to the processes. The electrolytes are recovered and recycled using membrane diafiltration.

An assumption often employed when modeling membrane processes is negligible water recovery. While this is convenient for modeling purposes, it does not represent practical large-scale operation. In fact, the desire to maximize water recovery is the ultimate goal for anyone working in the field of RO. The conventional RO system for seawater desalination can achieve a 40–50% recovery operating at 65 bar (199). As discussed earlier, the major hindrance in obtaining larger recoveries is the sharp increase in osmotic pressure associated with highly concentrated retentate streams. In addition, impurities are concentrated and may cause severe fouling at elevated levels. Turek and Dydo (199), Mohsen and co-workers (200), Drioli and co-workers (3) and several others have presented discussions on processes for high water recovery. The most promising work in this area is a hybrid process that combines NF, RO, and crystallization membrane crystallizer (MC). Crystallization can be used to further treat the retentate from an RO stream because it uses supersaturation to induce crystal growth. The products of MC are salt crystals and pure water. Thus, combination of NF, RO, and MC is especially attractive because it makes 100% water recovery possible, with the added benefit that the recovered crystals can be sold for profit, thereby lowering the associated cost of water. A simplified process schematic is shown in Fig. 13.

Enhanced Separations. Traditional membrane processes rely on the morphological (porosity, pore size, tortuosity) and chemical (hydrophobicity–hydrophilicity, charge) properties of polymeric materials to control the transport of chemical species across the membrane. Therefore, the ability to enhance separations will involve the manipulation of these factors. As discussed earlier, a popular method for controlling the chemical properties is the incorporation of polyelectrolytes, both through surface attachment and as gel phases. The potential of these tuneable separations is especially attractive in applications ranging from toxic metal removal to protein recovery.

More recent efforts to enhance separation capabilities have involved the use of nanoscale additives. The inclusion of nanoparticles within the membrane matrix can have one of three effects on a chemical species: (*1*) the flux is greatly reduced because of the increased tortuosity within the membrane matrix, (*2*) the species experiences strong electrochemical interactions with the particle, or (*3*) the species is consumed by reaction at the particle surface. The overall effect of all three is hindered diffusion of the species through the membrane.

The use of nanoparticles to increase membrane tortuosity has been used in the food and electronics packaging industries to slow the transport of oxygen into containers of sensitive products (201). In this case, the impact of the particle on diffusion is only through physical (size) effects. The insertion of particles into the polymer matrix forces twisting and bunching of the polymer chains near the particle. These denser regions will be much more difficult for diffusing species to pass through.

When dealing with polar and ionic species (eg, the case in most RO and NF applications), the charge interactions between the nanoparticles and diffusing species will play an important role in the observed separation. Depending on whether the interaction is attractive or repulsive, the diffusing species can be either strongly adsorbed to the particle surface and trapped within the membrane, or forced along a more tortuous charge-free path. In the field of pervaporation, Chandak and co-workers (202) examined the transport of chlorinated organics and ethanol vapors through DAY zeolite and silicalite filled polydimethylsiloxane (PDMS) membranes. They determined the diffusion coefficients for ethanol, trichloroethylene (TCE), and 1,1,1-trichloroethane (TCA) in these membranes at both 20 and 40 wt% particle loadings. This is an interesting case because the particles are both charged and porous, which means they will have both a physical and chemical effect on transport. The zeolites had the most impact on the transport of the polar ethanol molecules. Although the solubility of ethanol in the films was increased, its diffusivity greatly decreased as ethanol molecules became adsorbed to the charged zeolite surfaces. For the chlorinated organics, the zeolites served more as a sterical hindrance, limiting mobility of TCE and TCA molecules through the particle pore structures. The TCE was least affected because its double-bonded structure allowed it to more freely rotate and navigate the zeolite pores. This type of modified flux behavior could easily be extended to RO and NF applications involving the separation of organics. The use of membrane adsorbers for heavy metal recovery has already been considered.

The third type of interaction that nanoparticles can have with diffusing species is chemical reactions. In this case, the target species is not rejected, but transformed into a more desired product. The ability to separate the compound is a strong function of the membrane reactivity. If the reaction is noncatalytic, the target species will eventually breakthrough the membrane when all the immobilized reactant is consumed. In environmental applications, this idea has been explored extensively with the concept of reactive permeable barriers in groundwater treatment, mainly targeting chlorinated organics, polychlorobiphenyls (PCBs), and nitrates (203–205). As opposed to pump-and-treat methods involving adsorption and membrane processes, a reactive barrier composed of a zero-valent metal (normally Fe^0) is placed in the ground in contact with the surrounding water tables. As pollutants pass through the barrier, they are transformed into a less toxic forms. For example, Fe^0 reduces TCE to ethane.

The incorporation of this idea with traditional RO and NF separations provides an interesting alternative for the treatment of waste streams involving such compounds. Not only does this allow for the elimination of downstream processing steps, it also provides for the recovery of potentially valuable materials that could be recycled to cut process costs. The first step in developing such applications is to synthesize the materials necessary to accomplish this type of separation. Meyer and co-workers (206) demonstrated the ability to derive asymmetric CA films containing reactive nanoscale metal particles (Fe, Ni) using the phase inversion process (Fig. 14). These films have been used in batch experiments to destroy chlorinated organics (TCE = tetrachloroethane) in aqueous solutions (Fig. 15). They were able to achieve up to 80% reduction in TCE levels in < 2 h of reaction time. For practical purposes, the reaction time must first be shortened and their work has not yet studied the mechanical properties of these films for pressure-driven applications. Daub and co-workers (207) used modified ceramic MF and UF membranes for the denitrification of aqueous solutions. They used either chemical vapor deposition or surface impregnation to load Pd−Sn or Pd−Cu into the membranes. Nitrate was reduced in batch operation by these films to N_2. However, they did find that the formation of unwanted ammonium as a side reaction is a potential problem if better selectivity and activity cannot be achieved during synthesis.

Although this type of work is still in its infancy, it is easy to see how these films can be incorporated into an NF/RO process. For example, suppose a waste stream containing 3% salts, 1 mg/L of heavy metals, and 5 mg/L of a chlorinated organic must be treated for discharge. A simplified process is shown in Fig. 16. Floculation and precipitation can first be used to remove the metals in solid form. The remaining stream, containing the chlorinated organic and salt is then fed to a loose RO membrane containing Fe^0 nanoparticles. Although reductions in salt levels comparable to NF could be achieved using this membrane, its main purpose is to dechlorinate (detoxify) the chlorinated organic. The permeate from this unit is then fed to an RO unit for recovery of high purity water. If larger salt rejections are achieved during the reaction step, a high recovery of water is possible.

11. Acknowledgments

The authors recognize the U.S. EPA - STAR-2001 program, SBRP-NIEHS, NSF-IGERT, and NIST-ATP for the support of some the work presented in this paper. The authors like to thank Dr. Ritchie, Dr. Hestekin, Dr. Sikdar, and Dr. Bachas for their research contribution with the functionalized membrane work. We would also like to extend our sincere appreciation to Dr. Steve Kloos, Osmonics Corporation, for providing various data for the NF membranes and also for his contribution with the solvent resistant membrane work. The authors would also to thank William Mangum, Aaron Hollman, and Dharmesh Bhanushali for some of the data presented in this article. Hollman and Meyer were NSF-IGERT Fellows.

12. Nomenclature

A	Water permeability coefficient, L^3/L^2tP
A^*	Modified water permeability constant, L^3/L^2tP
$\tilde{A}$	Measure of electrostatic force between solute and pore wall, L
A_m	Membrane surface area, L^2
B	Solute permeability coefficient, t^{-1}
$\tilde{B}$	Measure of solute-membrane pore wall interaction force, L_3
B^*	Modified solute permeability constant, mol/L^2t
b_0	Sorption coefficient, L^3/mol
C_B	Bulk concentrate solute concentration, mol/L^3 or M/L^3
C_F	Feed solute concentration, mol/L^3 or M/L^3
C_m	Membrane solute concentration, mol/L^3
C_P	Permeate solute concentration, mol/L^3 or M/L^3
C_{tm}	Total concentration of water and solute in the membrane, mol/L^3
C_{wall}	Feed solute concentration at the membrane wall, mol/L^3 or M/L^3
C_{wm}	Membrane water concentration, mol/L^3
D_{sm}	Membrane solute diffusivity, L^2/t
D_{wm}	Membrane water diffusivity, L^2/t
F_F	Feed flow rate, L^3/t
F_P	Permeate flow rate, L^3/t
J_s	Solute flux, mol/L^2t or M/L^2t
J_w	Water flux, L^3/L^2t
J_{wo}	Pure water flux, L^3/L^2t
K_{sm}	Solute partition coefficient for homogeneous membrane, dimensionless
k_s	Mass transfer coefficient, L/t
ΔP	Transmembrane pressure difference, M/Lt^2
r	Permeate water recovery, dimensionless
R	Solute rejection, dimensionless
R_{int}	Intrinsic solute rejection, dimensionless
R_{obs}	Observed solute rejection, dimensionless
R_g	Ideal gas constant, $ML^2/t^2T\ mol$
R_p	Membrane pore radius, L
Re	Reynold's number, dimensionless
Sc	Schmidt number, dimensionless
Sh	Sherwood number, dimensionless
t	Time
T	Temperature
V_F	Feed volume, L^3
V_P	Permeate volume, L^3
V_w	Water permeation velocity, L/t
$\bar{V}\mathrm{w}$	Partial molar volume of water, L^3/mol
Greek Letters	
δ	Membrane thickness, L

$\Delta \pi$	Transmembrane osmotic pressure difference, M/Lt^2
σ	Staverman reflection coefficient, dimensionless
μ	Viscosity, M/Lt
μ_s	Solute chemical potential, E/mol
μ_w	Water chemical potential, E/mol
ρ	Density, M/L^3
Abbreviations	
AFM	Atomic force microscopy
BOD	Biological oxygen demand
CA	Cellulose acetate
CP	Concentration polarization
COD	Chemical oxygen demand
DBP	Disinfection by-products
edta	Ethylenediaminetetraacetato
FT30-BW	Dow/*FilmTec aromatic polyamide composite reverse osmosis membrane*
NF	Nanofiltration
MC	Membrane crystallizer
MF	Microfiltration
MSD	Modified solution diffusion
MSF	Multistage flash
NOM	Natural organic matter
PA	Polyamide
RO	Reverse osmosis
SD	Solution-diffusion
SFPF	Surface force-pore flow
TDS	Total dissolved solids
TFC	Thin-film composite
THM	Trihalomethane
TOC	Total organic carbon
UF	Ultrafiltration
ULP	Ultralow pressure

BIBLIOGRAPHY

"Osmosis and Osmotic Pressure" in *ECT* 1st ed., Vol. 9, pp. 643–660, by E. H. Immergut and K. G. Stern, Institute of Polymer Research, Polytechnic Institute of Brooklyn; "Osmosis, Osmotic Pressure, and Reverse Osmosis" in *ECT* 2nd ed., Vol. 14, pp. 345–356, by B. Keilin, Amicon Corp.; "Reverse Osmosis" in *ECT* 3rd ed., Vol. 20, pp. 230–248, by J. S. Johnson, Jr., Oak Ridge National Laboratory; in *ECT* 4th ed., Vol. 21, pp. 303–335, by D. Bhattacharyya and W. C. Mangum, University of Kentucky, and M. E. Williams, EET Corp.; "Reverse Osmosis" in *ECT* (online), posting date: December 4, 2000, by D. Bhattacharyya and W. C. Mangum, University of Kentucky, and M. E. Williams, EET Corp.

1. B. Van der Bruggen, L. Lejon, and C. Vandecasteele. *Env. Sci. Tech.* **37**(17), 3733 (2003).

2. R. J. Petersen, *J. Membrane Sci.* **83**, 81 (1993).
3. E. Drioli, A. Criscuoli, and E. Curcio, *Desalination* **147**, 77 (2002).
4. C. Reid and E. Breton, *J. Appl. Polym. Sci.* **1**, 133 (1959).
5. P. Ferguson, *Desalination* **32**, 5 (1980).
6. H. Lonsdale, *J. Membrane Sci.* **10**, 81 (1982).
7. L. Applegate, *Chem. Eng.* **64** (June 11, 1984).
8. S. Loeb and S. Sourirajan, *Adv. Chem. Ser.* **38**, 117 (1962).
9. S. Loeb, The Loeb-Sourirajan Membrane: How it Came About, in A. Turbak, ed., *Synthetic Membranes*, Vol. 1, ACS Symposium Series 153, Washington, D.C., 1981.
10. S. Sourirajan and T. Matsuura, *Reverse Osmosis / Ultrafiltration Principles*, National Research Council of Canada, Ottawa, Canada, 1985.
11. D. Bhattacharyya and co-workers, in W. Ho and K. Sirkar, eds., *Membrane Handbook*, Van Nostrand Reinhold, New York, 1992, pp. 263–390.
12. E. Drioli and M. Romano, *Ind. Eng. Chem. Res.* **40**, 1277 (2001).
13. R. Riley, Reverse Osmosis, in Membrane Separation Systems **2**, US DOE Report, DOE/ER/30133-H1, 1990.
14. www.mcilvainecompany.com/news%20releases/NR823.htm (2003).
15. B. Parekh, ed., *Reverse Osmosis Technology*, Marcell Dekker, Inc., New York, 1988.
16. G. Belfort, ed., *Synthetic Membrane Processes: Fundamentals and Water Applications*, Academic Press, New York, 1984.
17. D. Lloyd and T. Meluch, Selection and Evaluation of Membrane Materials for Liquid Separations, ACS Symposium Series No. 269, Washington, D.C., 1985.
18. R. Rautenbach and R. Albrecht, *Membrane Processes*, John Wiley & Sons, Inc., New York, 1989.
19. J. Howell, V. Sanchez, and R. Field, eds., *Membranes in Bioprocessing: Theory and Applications*, Chapman and Hall, New York, 1993.
20. R. Kesting, *Synthetic Polymeric Membranes: A Structural Perspective*, Wiley-Interscience, New York, 1985.
21. I. Cabasso, *Encyclopedia of Polymer Science and Engineering*, Vol. 9, John Wiley & Sons, Inc., New York, 1987, pp. 509–579.
22. W. Koros and co-workers, *Prog. Polym. Sci.* **13**, 339 (1988).
23. R. Baker, Membrane and Module Preparation, in Membrane Separation Systems **2**, US DOE Report, DOE/ER/30133-H1, 1990.
24. H. Strathmann, in M. Porter, ed., *Handbook of Industrial Membrane Technology*, Noyes Publications, Park Ridge, N.J., 1990, pp. 1–60.
25. R. Petersen and J. Cadotte, **20**, 307 (1990).
26. V. Freger, *Environ. Sci. Tech.* **38** (11), 3168 (2004).
27. N. Hilal and co-workers, *Desalination* **170**, 281 (2004).
28. S. Kwak, S. Jung, and S. Kim, *Environ. Sci. Tech.* **35** (21), 4334 (2001).
29. S. Kwak, S. H. Kim, and S. S. Kim, *Environ. Sci. Tech.* **35** (11), 2388 (2001).
30. P. Stanford, Open-Channel Membrane Modules for the Reduction of Hazardous Liquids, Proceedings of the North American Membrane Society Conference, Portland, Or., 1995.
31. T. Peters, *Desalination* **83**, 159 (1991).
32. J. Marriott and E. Sorensen, *Chem. Eng. Sci.* **58**, 4975 (2003).
33. A. von Gottberg, *Filtration Separation* 32 (2004).
34. V. Gekas, *Desalination* **68**, 77 (1988).
35. G. Jonsson, *Desalination* **35**, 21 (1980).
36. M. Soltanieh and W. Gill, *Chem. Eng. Comm.* **12**, 279 (1981).
37. M. Mazid, *Sep. Sci. Technol.* **19**, 357 (1984).
38. W. Pusch, *Desalination* **59**, 105 (1986).
39. H. Lonsdale, U. Merten, and R. Riley, *J. Appl. Polym. Sci.* **9**, 1341 (1965).

40. H. Burghoff, K. Lee, and W. Pusch, *J. Appl. Polym. Sci.* **25**, 323 (1980).
41. J. Dickson in Ref. 15.
42. D. Paul, *J. Membrane Sci.* **241**, 371 (2004).
43. T. Matsuura and S. Sourirajan, *Ind. Eng. Chem. Process Des. Dev.* **20**, 273 (1981).
44. H. Mehdizadeh and J. Dickson, *J. Membrane Sci.* **42**, 119 (1989).
45. H. Mehdizadeh, Modeling of Transport Phenomena in Reverse Osmosis Membranes, Dissertation, J. Dickson, Director, Department of Chemical Engineering, McMaster University, Hamilton, Ontario, Canada, 1990.
46. H. Mehdizadeh and J. Dickson, *Comp. Chem. Eng.* **14**, 157 (1990).
47. D. Bhattacharyya and co-workers, *Chem.Eng. Comm.* **42**, 111 (1986).
48. J. Siler, Reverde Osmosis Membranes-Concentration Polarization and Surface Fouling: Predictive Models and Experimental Verifications, Dissertation, D. Bhattacharyya, Director, Department of Chemical Engineering, University of Kentucky, Lexington, Ky., 1987.
49. E. Matthiasson and B. Sivik, *Desalination* **35**, 59 (1980).
50. V. Gekas and B. Hallstrom, *J. Membrane Sci.* **30**, 153 (1987).
51. D. Bhattacharyya, S. Back, and R. Kermode, *J. Membrane Sci.* **48**, 231 (1990).
52. P. Brian, in U. Merten, ed., *Desalination by Reverse Osmosis*, MIT Press, Cambridge, Mass., 1966, pp. 161–202.
53. M. Williams, Ph.D. dissertation, Measurement and Mathematical Description of Separation Characteristics of Hazardous Organic Compounds with Reverse Osmosis Membranes, Department of Chemical Engineering, University of Kentucky, Lexington, Ky., 1993.
54. B. Durham, M. Bourbigot, and T. Pankratz, *Desalination* **138**, 83 (2001).
55. A. Helal and co-workers, *Desalination* **169**, 43 (2004).
56. T. Matsuura, *Desalination* **134**, 47 (2001).
57. S. Agashichev and A. El-Nashar, *Energy* **30**, 1283 (2005).
58. O. Bouhelal, R. Merrouch, and D. Zejli, *Desalination* **165**, 251 (2004).
59. E. Cardona and A. Piacentino, *Desalination* **166**, 411 (2004).
60. L. Awerbuch and co-workers, *Desalination* **76**, 189 (1989).
61. E. Lohman, *Desalination* **96**, 349 (1994).
62. Y. Ayyash and co-workers, *Desalination* **96**, 215 (1994).
63. P. Cartwright, *Desalination* **56**, 17 (1985).
64. J. Schoeman and co-workers, *Water Sci. Tech.* **25**, 79 (1992).
65. C. Slater, J. Zielinski, and R. Wendel, *J. Environ. Sci. Health* **A27**(5), 1175 (1992).
66. J. Castelblanque and F. Salimbeni, *Desalination* **167**, 65 (2004).
67. J. Qin and co-workers, *J. Membranes Sci.* **208**, 213 (2002).
68. C. Schmidt, I. White, and R. Ludwig, EPA Report, EPA/600/R-93/150, 1993.
69. K. Imasu, *Desalination* **56**, 137 (1985).
70. T. Thorsen, *Desalination* **53**, 217 (1985).
71. G. Hsiue, L. Pung, M. Chu, and M. Shieh, *Desalination* **71**, 35 (1989).
72. M. Chu, C. Tung, and M. Shieh, *Sep. Sci. Technol.* **25**, 1339 (1990).
73. S. Prabhakar and co-workers, *Separation Sci. Technol.* **27**, 349 (1992).
74. S. Prabhakar and co-workers, *Separation Sci. Technol.* **29** (8), 1001 (1994).
75. J. Arnal and co-workers, *Desalination* **154**, 27 (2003).
76. J. Arnal and co-workers, *Desalination* **154**, 35 (2003).
77. G. Zakrzewska-Trznadel, M. Harasimowicz, and A. Chmielewski, *Separation Purification Technol.* **22–23**, 617 (2001).
78. R. Rautenbach and R. Mellis, *Desalination* **101**, 105 (1995).
79. K. Linde, A-s. Jönsson, and R. Wimmerstedt, *Desalination* **101**, 21 (1995).
80. AWWA Membrane Technology Research Committee, *J. AWWA*, 59 (January 1992).
81. T. Marhaba and S. Medler, *Proc. 1994 Natl. Conf. Env. Eng.* 476 (1994).

82. L. Tan and R. Sudak, *J. AWWA* **84**, 79 (1992).
83. T. Eisenberg and E. Middlebrooks, *Reverse Osmosis Treatment of Drinking Water*, Butterworth, Boston, 1986.
84. J. Jacangelo and co-workers, *J. AWWA* **87**, 64 (1995).
85. S. Ritchie and D. Bhattacharyya, *J. Hazardous Materials* **92**, 21 (2002).
86. S. Ritchie and co-workers, *Environ. Sci. Tech.* **35**(15), 3252 (2001).
87. H. Qdais and H. Moussa, *Desalination* **164**, 105 (2004).
88. I. Atamanenko and co-workers, *Desalination* **158**, 151 (2003).
89. H. Ozaki, K. Sharma, and W. Saktaywin, *Desalination* **144**, 287 (2002).
90. H. Tsuge and K. Mori, *Desalination* **23**, 123 (1977).
91. I. Nusbaum and D. Argo in Ref. 16.
92. M. Reinhard and co-workers, *J. AWWA*, 163 (April 1986).
93. Y. Suzuki and T. Minami, *Water Sci. Tech.* **23**, 1629 (1991).
94. S. Kim, J. Chen, and Y. Ting, *Sep. Pur. Tech.* **29**, 171 (2002).
95. J. Schaefer, *Desalination* **138**, 91 (2001).
96. M. Clever and co-workers, *Desalination* **131**, 325 (2000).
97. C. Frith in Ref. 15.
98. D. Ulieru, Proceedings of the 19th Annual Technical Meeting of Inst. of Environmental Science, Las Vegas, Nev., 1993, pp. 186–191.
99. T. Ikeda, H. Muragishi, and T. Uemura, *Desalination* **98**, 391 (1994).
100. M. Okazaki and co-workers, *Desalination* **131**, 65 (2000).
101. Y. Egozy, J. Denoncourt, and G. Ganzi in Ref. 15.
102. P. Parise, B. Parekh, and R. Smith in Ref. 15.
103. B. Jiao, A. Cassano, and E. Drioli, *J. Food Eng.* **63**, 303 (2004).
104. P. Sinisgalli and J. McNutt, *J. AWWA*, 47 (May 1986).
105. P. Cartwright, *Desalination* **83**, 225 (1991).
106. C. Slater, R. Ahlert, and C. Uchrin, *Desalination* **48**, 171 (1983).
107. A. Ghabris, M. Abdel-Jawad, and G. Aly, *Desalination* **75**, 213 (1989).
108. M. El-Halwagi, *AIChE J.* **38** (8), 1185 (1992).
109. F. Awadalla, C. Striez, and K. lAMB, *Separation Sci. Technol.* **29**, 483 (1994).
110. A. Kulkarni, D. Mukherjee, and W. Gill, *Chem. Eng. Comm.* **129**, 53 (1994).
111. E. Chian and F. De Walle, EPA Report, EPA-600/2-77-186b, 1977.
112. C. Slater, R. Ahlert, and C. Uchrin, *Environ. Prog.* **2**, 251 (1983).
113. R. Kinman and D. Nutini, Treatment of Landfill Leachate Using Reverse Osmosis, Paper Presented at the 1990 International Congress on Membranes and Membrane Processes, August 20-24, 1990, Chicago, Ill.
114. D. Bhattacharyya and A. Kothari, A., Separation of Hazardous Organics by Low Pressure Membranes: Treatment of Soil-Wash Rinse-Water Leachates, EPA Report, Cooperative Agreement No. CR814491, 1992.
115. J. Lepore and R. Ahlert, *Waste Management* **11**, 27 (1991).
116. K. Ushikoshi and co-workers, *Desalination* **150**, 121 (2002).
117. J. Bohdziewicz, M. Bodzek, and J. Górska, *Proc. Biochem.* **36**, 641 (2001).
118. J. Meier, T. Melin, and L. Eilers, *Desalination* **146**, 361 (2002).
119. M. Nyström, L. Kaipia, and S. Luque, *J. Membrane Sci.* **98**, 249 (1995).
120. P. Eriksson, *Environ. Prog.* **7**, 58 (1988).
121. J. Cadotte and co-workers, *Desalination* **70**, 77 (1988).
122. G. Zakrzewska-Trznadel, *J. Membrane Sci.* **225**, 25 (2003).
123. A. Hollman and D. Bhattacharyya, *Langmuir* **20**, 5418 (2004).
124. W. Jin, A. Toutianoush, and B. Tieke, *Langmuir* **19**, 2550 (2003).
125. A. Mika and R. Childs, *Ind. Eng. Chem. Res.* **42**, 3111 (2003).
126. B. Stanton and co-workers, *Langmuir* **19**, 7038 (2003).
127. M. Miller and M. Bruening, *Langmuir* **20**, 11545 (2004).

128. S. de Lint and N. Benes, *J. Membrane Sci.* **243**, 365 (2004).
129. L. Raman, M. Cheryan, and N. Rajagopalan, *Chem. Eng. Prog.* **90** (3), 68 (1994).
130. L. Nghiem, A. Schafer, and M. Elimelech, *Environ. Sci. Tech.* **38** (6), 1888 (2004).
131. K. Košutić and co-workers, *Separation Purification Technol.* **42**, 137 (2005).
132. T. Gotoh, H. Iguchi, and K. Kikuchi, *Biochem. Eng. J.* **19**, 165 (2004).
133. A. Zhu and co-workers, *Water Res.* **37**, 3718 (2003).
134. W. Bowen and co-workers, *J. Membrane Sci.* **242**, 211 (2004).
135. J. Warczok and co-workers, *J. Food Eng.* **63**, 63 (2004).
136. A. Bindoff and co-workers, *Desalination* **67**, 453 (1987).
137. K. Ikeda and co-workers, *Desalination* **68**, 109 (1988).
138. M. Afonso and co-workers, *Water Res.* **26**, 1639 (1992).
139. M. Simpson, C. Kerr, and C. Buckley, *Desalination* **64**, 305 (1987).
140. M. Perry and C. Linder, *Desalination* **71**, 233 (1989).
141. Anonymous, *Food Eng.* **60**, 124 (1988).
142. P. Fu, H. Ruiz, K. Thompson, and C. Spangenberg, *J. AWWA* **86**(12), 55 (1994).
143. K. Agbekdo and co-workers, *Rev. Sci. Eau* **7**(2), 183 (1994).
144. R. Rautenbach and R. Mellis, *Desalination* **95**, 171 (1994).
145. D. Bhattacharyya, R. Adams, and M. Williams, in D. Butterfield, ed., *Biological and Synthetic Membranes*, Alan R. Liss, New York, 1989.
146. M. Williams, R. Deshmukh, and D. Bhattacharyya, *Environ. Prog.* **9**, 118 (1990).
147. D. Bhattacharyya and M. Williams, EPA Report, EPA/600/2-91/045, 1992.
148. C. Dyke and C. Bartels, *Environ. Prog.* **9**, 183 (1990).
149. A. Hollman and D. Bhattacharyya, *Langmuir* **18**, 5946 (2002).
150. R. Childs and A. Mika, in D. Bhattacharyya and D. Butterfield, eds., *New Insights into Membrane Science and Technology: Polymeric and Biofunctional Membranes*, Elsevier Sciences B. V., 2003.
151. S. L. White and A. R. Nitsch, *J. Membrane Sci.* **179**, 267 (2000).
152. R. M. Gould, S. L. White, and C. R. Wildemuth, *Environ. Prog.* **20**, 12 (2001).
153. J. T. Scarpello and co-workers, *J. Membrane Sci.* **203**, 71 (2002).
154. D. R. Machado, D. Hasson, and R. Semiat, *J. Membrane Sci.* **163**, 93 (1999).
155. D. Bhanushali, D. Bhattacharyya, and S. D. Kloos, *J. Membrane Sci.* **208**, 343 (2002).
156. D. Bhanushali and co-workers, *J. Membrane Sci.* **189**, 1 (2001).
157. G. H. Koops, S. Yamada, and S.-I. Nakao, *J. Membrane Sci.* **189**: 241 (2001)
158. S. S. Luthra and co-workers, *Chem. Commun.* **16**: 1468 (2001).
159. C. Bellona and co-workers, *Water Res.* **38**, 2795 (2004).
160. S. Sourirajan, *Reverse Osmosis*, Academic Press, New York, 1970.
161. K. Košutić and B. Kunst, *Desalination* **142**, 47 (2001).
162. K. Agenson, J. Oh, and T. Urase, *J. Membrane Sci.* **225**, 91 (2003).
163. C. Schutte, *Desalination* **158**, 285 (2003).
164. H. Ozaki and H. Li, *Water Res.* **36**, 123 (2002).
165. J. Jiang and co-workers, *Desalination* **17**, 107 (1989).
166. S. Gao and Q. Bao, *J. Liquid Chromatog.* **12**, 2083 (1989).
167. J. Jiang and C. Jiayan, *Desalination* **78**, 389 (1990).
168. R. Rautenbach and A. Gröschl, Fractionation of Aqueous Organic Mixtures by Reverse Osmosis, Paper Presented at 203rd American Chemical Society National Meeting, April 5-10, 1992, San Francisco, Calif.
169. J. Weißbrodt and co-workers, *Desalination* **133**, 65 (2001).
170. E. Hoek and M. Elimelech, *Environ. Sci. Tech.* **37** (24), 5581 (2003).
171. X. Zhu and M. Elimelech, *Environ. Sci. Tech.* **31** (12), 3654 (1997).
172. H. Ridgway in Ref. 15.
173. H. Ridgway, M. Rigby, and D. Argo, *J. AWWA* **77**, 97 (1985).

174. B. Van der Bruggen and C. Vandecasteele, *Desalination*, **143**, 207 (2002).
175. J. Lepore and R. Ahlert in Ref. 15.
176. T. Osta and L. Bakheet, *Desalination* **63**, 71 (1987).
177. S.N. Gaeta and co-workers, *Desalination*, **83**, 383 (1991).
178. K. Nita and co-workers, *Desalination* **96**, 33 (1994).
179. R. Singh, *Desalination*, **95**, 27 (1994).
180. J. Glater, S-k. Hong, and M. Elimelech, *Desalination*, **95**, 325 (1994).
181. G. Congjie, L. Xueren, and B. Zhiguo, *Desalination*, **83**, 271 (1991).
182. A. Ko and D. Guy in Ref. 15.
183. J. Redondo, *Desalination* **138**, 29 (2001).
184. S. Ebrahim, *Desalination* **96**, 225 (1994).
185. S. Ebrahim and H. El-Dessouky, *Desalination* **99**, 169 (1994).
186. A. Jaffer, *Desalination* **96**, 71 (1994).
187. Q. Li, M. Elimelech, *Environ. Sci. Tech.* **38** (17), 4683 (2004).
188. C. Brouckaert and C. Buckley, *Water SA* **18**(3), 215 (1992).
189. A. Malek, M. Hawlader, and J. Ho, *Desalination* **99**, 19 (1994).
190. R. Ray, in W. Ho and K. Sirkar, eds., **9**, 355 (1992).
191. H. Niemi and S. Palosaari, *J. Membrane Sci.* **84**, 123 (1993).
192. A. Mohammad and co-workers, *Desalination* **165**, 243 (2004).
193. B. Van der Bruggen and co-workers, *J. Membrane Sci.* **193**, 239 (2001).
194. J. Brant and A. Childress, *J. Membrane Sci.* **241**, 235 (2004).
195. J. Gilron and co-workers, *Desalination* **140**, 167 (2001).
196. M. Luo and co-workers, Appl. Surface Sci. in Press.
197. M. Saad, *Desalination* **165**, 183 (2004).
198. C. Allegre and co-workers, *Desalination* **162**, 13 (2004).
199. M. Turek and P. Dydo, *Desalination* **157**, 51 (2003).
200. M. Mohsen, J. Jaber, and M. Afonso, *Desalination* **157**, 167 (2003).
201. C. Yang, E. Nuxoll, and E. Cussler, *AIChE Journal* **47**, 295 (2001).
202. M. Chandak and co-workers, *J. Membrane Sci.* **133**, 231 (1997).
203. J. Szecsody and co-workers, *Environ. Sci. Tech.* **38**, 4656 (2004).
204. J. Klausen and co-workers, *Environ. Sci. Tech.* **37**, 1208 (2003).
205. S. Yabusaki and co-workers, *Environ. Sci. Tech.* **35**, 1493 (2001).
206. D. Meyer and co-workers, *Environ. Prog.* **23**, 232 (2004).
207. K. Daub and co-workers, *Chem. Eng. Sci.* **54**, 1577 (1999).

D. E. MEYER
M. WILLIAMS
D. BHATTACHARYYA
University of Kentucky Lexington

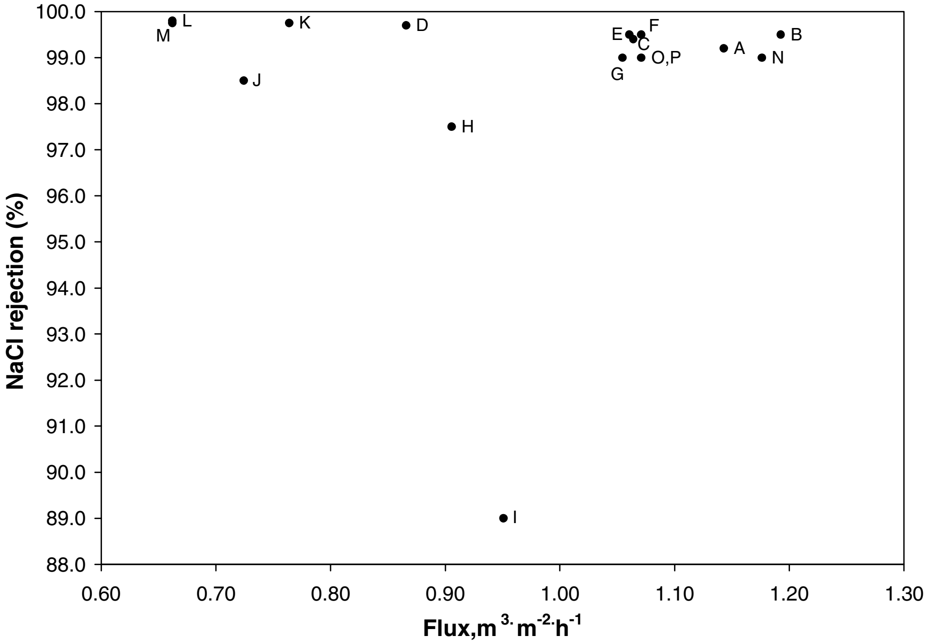

Fig. 1. Water flux and NaCl rejections for the following commercial RO membranes: **A** = Dow FT BW30LE-4040, **B** = Dow FT BW30-4040, **C** = GE Osmonics AG4040F, **D** = Hydranautics CPA4, **E** = Toray TM720-365, **F** = GE Osmonics OSMO MUNI RO-350, **G** = AMI M-B4040A, **H** = GE Osmonics CG4040F, **I** = GE Osmonics CE4040F, **J** = GE Osmonics CD4040F, **K** = Dow FT SW30HR-320, **L** = Hyrdanautics SWC4+, **M** = Toray TM820-400, **N** = Dow FT XLE-440, **O** = GE Osmonics OSMO MUNI LE-RO-350, **P** = GE Osmonics OSMO BEV RO. For BWRO membranes (**A**–**J**), $C_F = 2000$ mg/L and $\Delta P = 15.5$ bar, except for **A** ($\Delta P = 10.3$ bar) and **I**–**J** ($\Delta P = 29.3$ bar). For SWRO membranes (**K**–**M**), $C_F = 2000$ mg/L and $\Delta P = 55.2$ bar. For **N**–**P** (specialty applications: low pressure, food and beverage), $C_F = 2000$ mg/L and $\Delta P = 6.9$ bar (**N**), 7.9 bar (**O**), 15.5 bar (**P**). All information is available through manufacturers' websites.

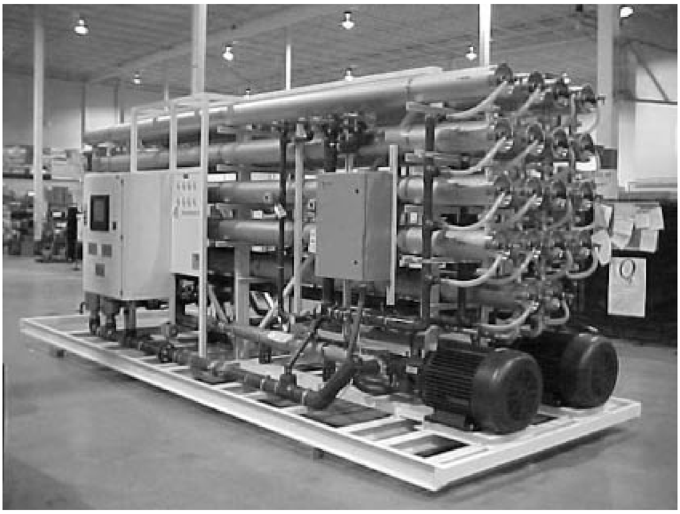

Fig. 2. A photo of a typical full-scale RO membrane module (spiral-wound) system capable of producing 500,000 gal/day (1892.7 m^3/day). *Note*: Each tube (pressure vessel) contains six spiral wound modules. (Courtesy of GE Osmonics.)

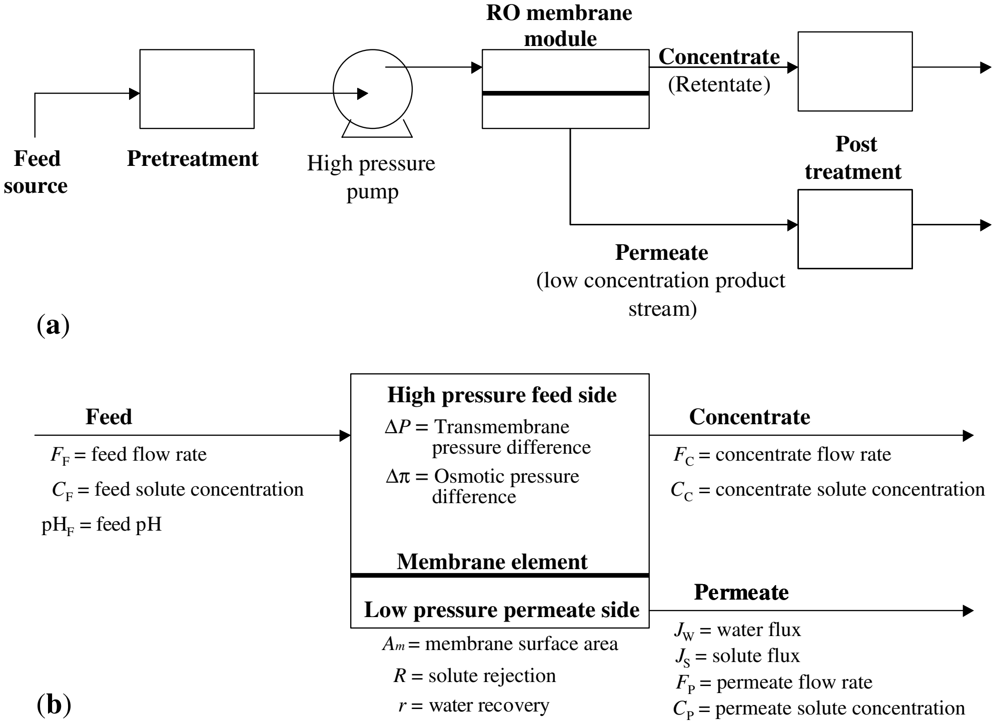

Fig. 3. Schematic of (**a**) a simplified RO membrane process and (**b**) the RO process streams.

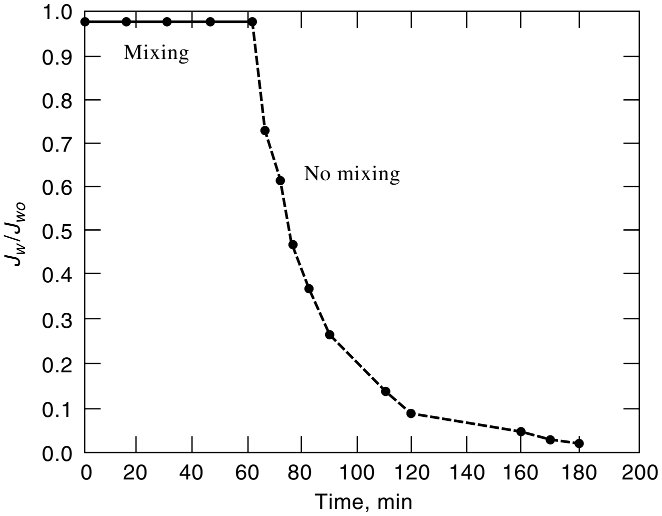

Fig. 4. A comparison of flux data (expressed as J_w/J_{wo}) obtained for the treatment of a $CaSO_4$ solution using an FT30-BW membrane operated with and without mixing to demonstrate the effect of concentration polarization and precipitation.

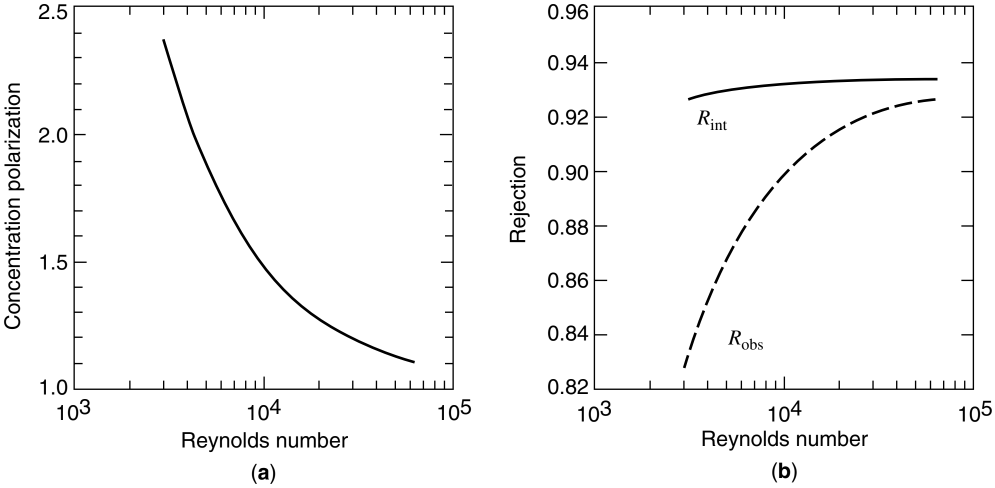

Fig. 5. Use of the film theory model to simulate the impact of feed velocity (as represented by variations in Re) on: (**a**) the concentration polarization factor (CP), and (**b**) the observed and intrinsic rejections, R_{obs} and R_{int}.

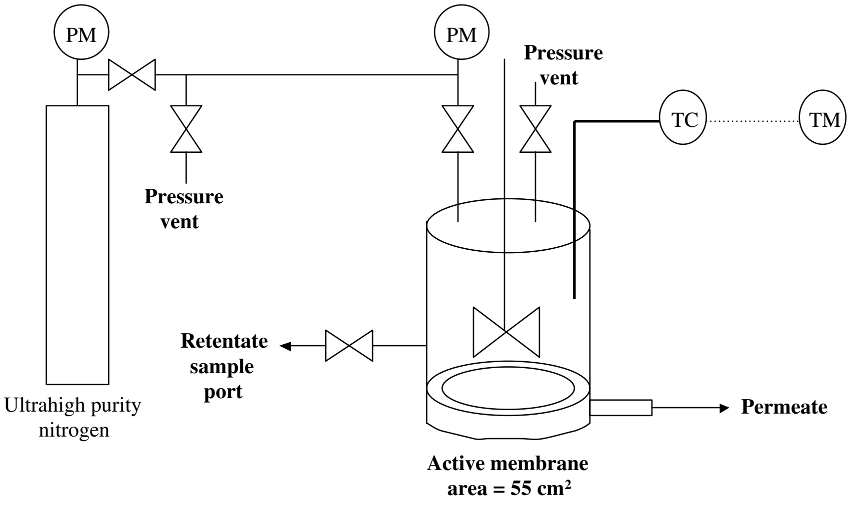

PM = Pressure Meter, TM = Temperature Meter, TC = Thermocouple

Fig. 6. A schematic of a stirred batch RO unit pressurized using compressed nitrogen.

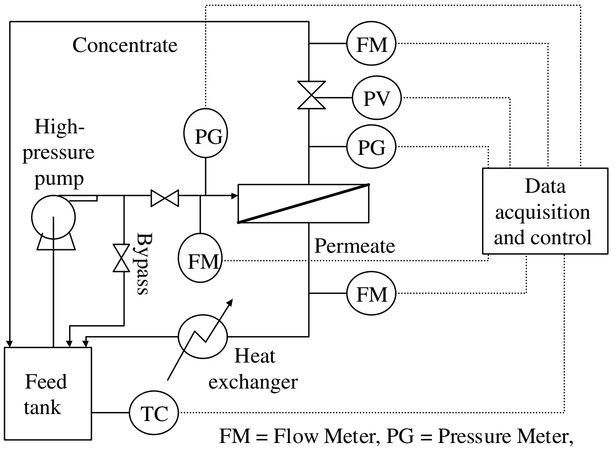

FM = Flow Meter, PG = Pressure Meter,
PV = Pressure Control Valve, TC = Thermocouple

Fig. 7. A schematic of a computer-controlled, continuous labscale RO unit pressurized by a pump.

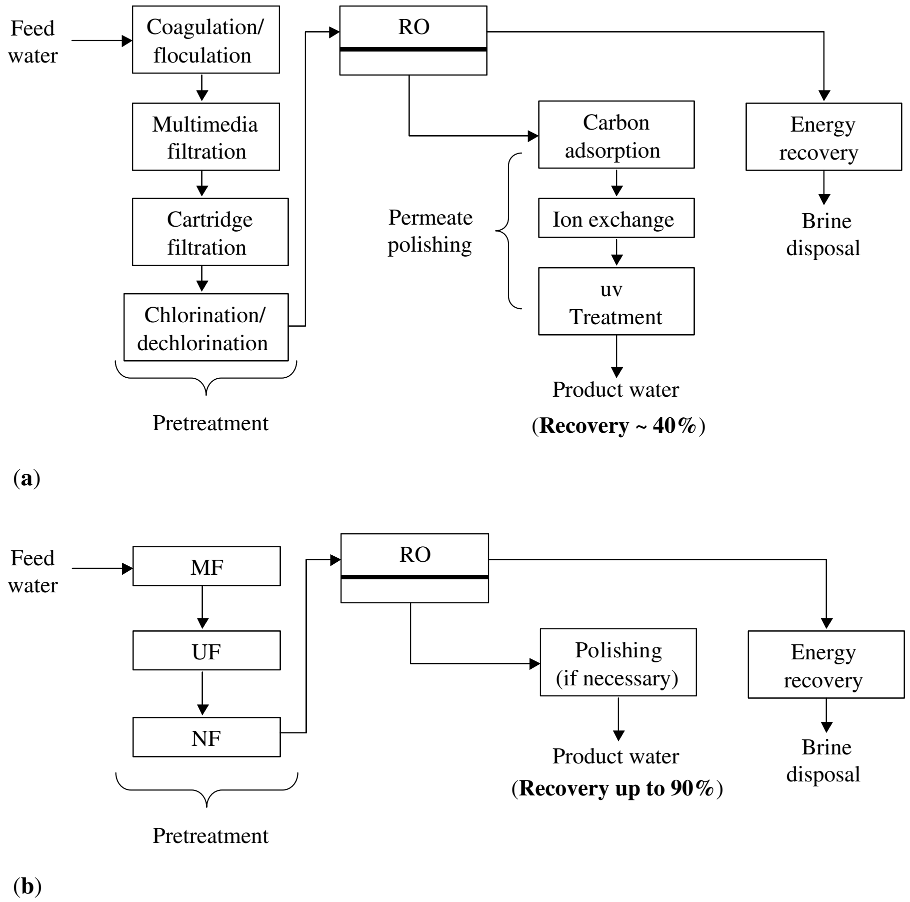

Fig. 8. A full-scale desalination process involving: (**a**) conventional pretreatment, and (**b**) membrane filtration pretreatment (MF, UF, and NF).

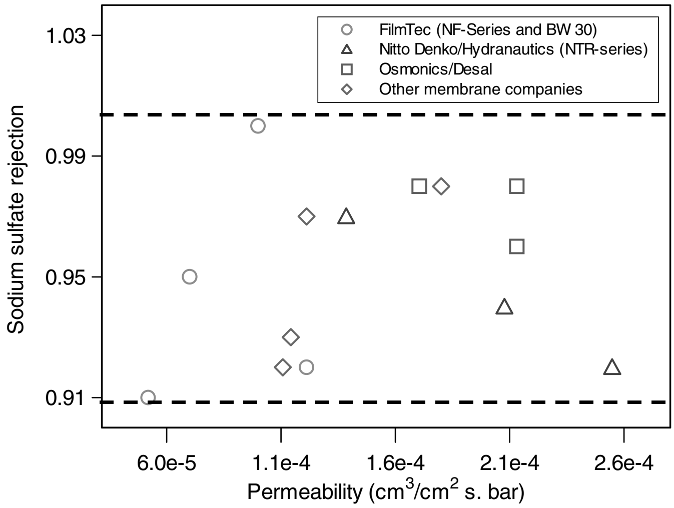

Fig. 9. Water permeability and SO_4^{2-} rejection for several commercial NF membranes. The data was obtained from manufacturers' websites.

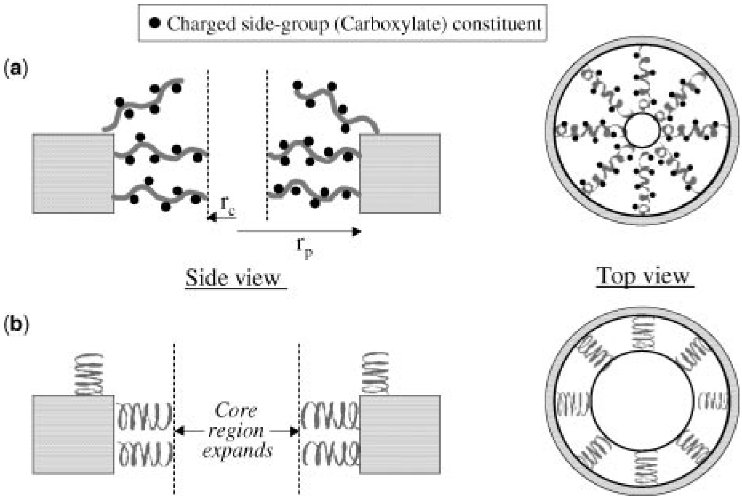

Fig. 10. Schematic of the helix-coil transition within the pore of a PLGA functionalized membrane; (**a**) random-coil formation at pH > 5.5, (**b**) helix formation at low pH (< 4). r_p = membrane pore radius; $r_c = r_p$ − PLGA chain length.

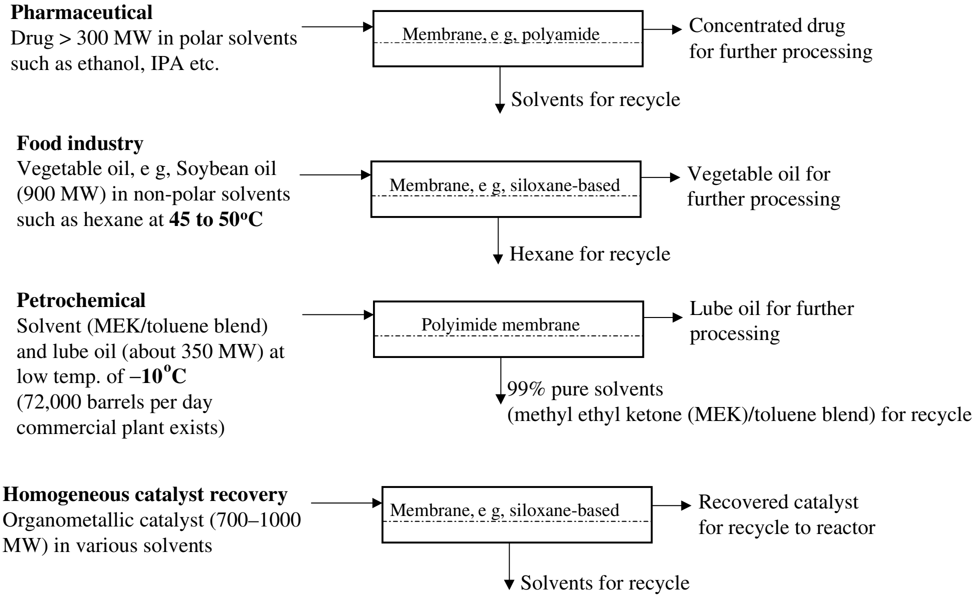

Fig. 11. Use of solvent-resistant membranes for material recovery and solvent recycle.

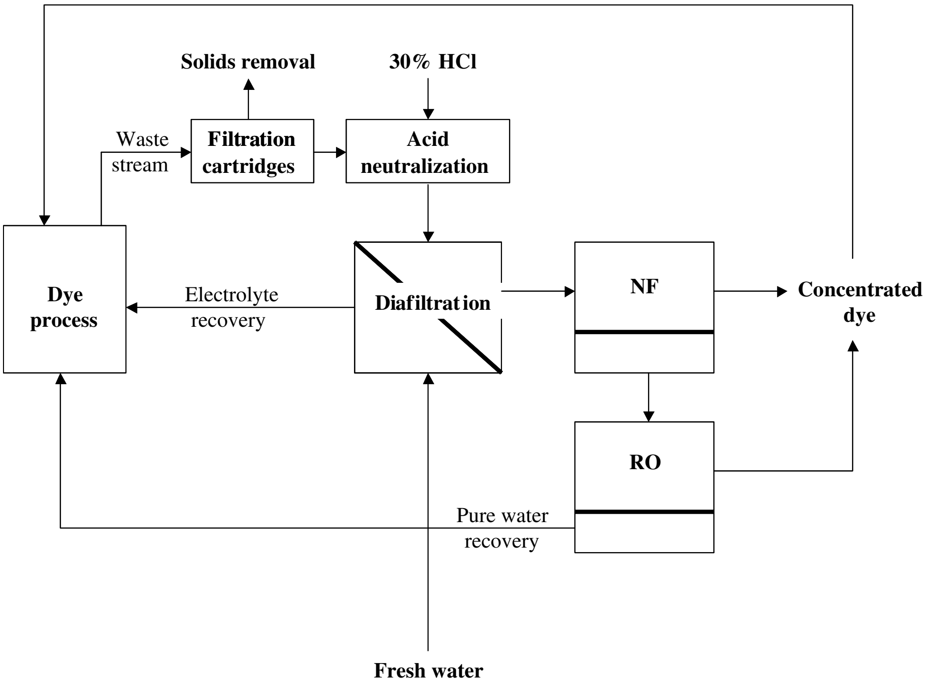

Fig. 12. The recovery and reuse of dyes from a textile waste stream containing cotton fibers, dyes, and dissolved salts using a hybrid filtration process.

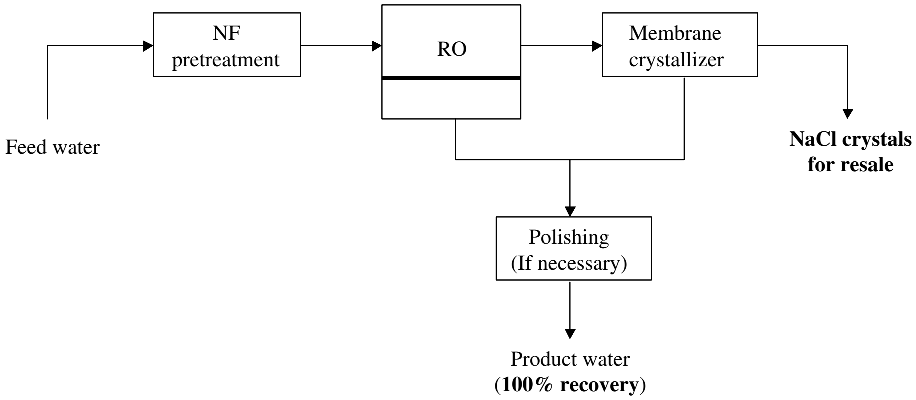

Fig. 13. A schematic of the NF-RO-MC process used to obtain 100% water recovery during desalination.

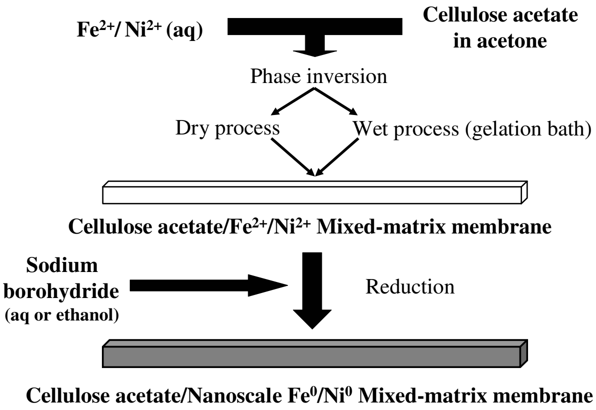

Fig. 14. Preparation of an asymmetric cellulose acetate (CA) film containing 1wt% reactive Fe/Ni bimetallic nanoparticles using the phase inversion synthesis technique.

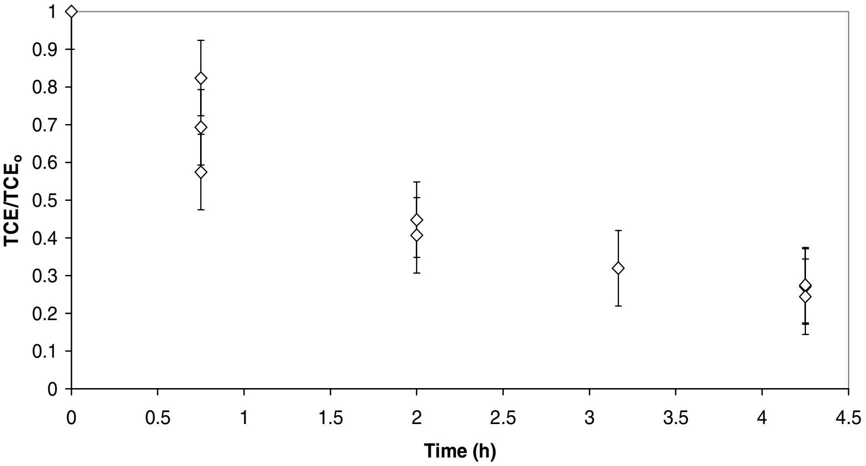

Fig. 15. Batch dechlorination of TCE using CA films containing Fe/Ni nanoparticles. The final product is ethane, as confirmed by gas chromatography.

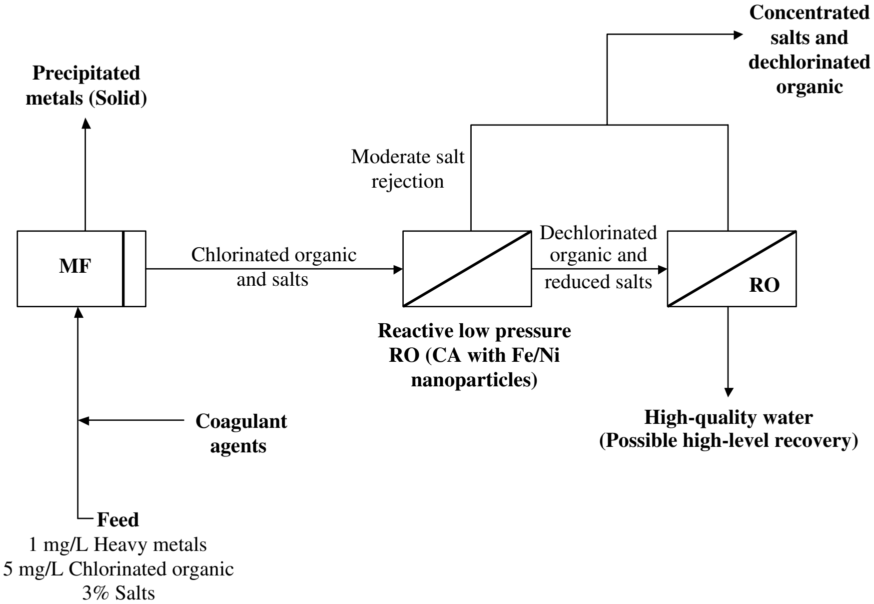

Fig. 16. A hypothetical hybridized process for the treatment of a waste stream containing 3% salts, 1 mg/L of heavy metals, and 1 mg/L of a chlorinated organic. The process involves a combination of flocculation–precipitation with MF to recover the metals, reactive low pressure RO for softening and to destroy the chlorinated organic, and RO for high quality water recovery.

Table 1. **Acid Resistant Nanofiltration (NF) and RO Membranes**

			2000 mg.L^{-1} Ionic rejection, (%)		Organic rejection, (%)[a]		
Osmonics membrane	Application type	Permeability $\times 10^3$ mh^{-1} bar^{-1}	NaCl	$MgSo_4$	61 MW	80 MW	Acid tolerance
AG (7–14 bar)[a]	RO	3.6	99.4	99.5 +	90	99	1
AK (7–14 bar)[b]	LPRO	6.0	99	99.5 +	80	99	1
Acid K (<69 bar)[c]	NF	3.2	80	99.50	60	95	see below
DK (7–14 bar)[b]	NF	7.1	50	99.50	10	95	1.5

[a] Organic rejection is for neutral unchanged organic species.

[b] Typical operating pressure ranges.

[c] Maximum operating pressure. The Acid K membrane is stable to 20% sulfuric acid at 50°C.

Table 2. **Selected Applications of Reverse Osmosis**

Application	References
desalination	12, 102–110
wastewater treatment	
electroplating	54–70
radioactive processing	71–77
landfill leachate	3, 61, 78, 79
drinking water/ municipal wastewater	3, 54, 80–95, 102
ultrapure water production	
electronics grade	96–100
laboratory grade	101
pharmaceutical grade	102
food and beverage	103

Table 3. **Typical Rejection of Organics by RO and NF Membranes with Varying Salt Rejections**

	Membrane Rejection (%)								
Manufacturer	N/A	N/A	Dow Danmark A/S	Fluid systems Corp.	Hydranautics	TriSep Corp.	Toray	Nitto	Nitto
Model No.	TFC	Assymetric	HR95PP	TFC-8821ULP	CPA2	TS80	UTC60	NTR729HF	ES10C
material	Aromatic PA	CA		PA			Aromatic PA	PVA/PA	PA
type	RO	RO	RO	ULPRO	ULPRO	NF	NF	NF	NF
Target Species									
NaCl	>97%	>97%	97.7	92.6	96	89.9	55	92	99.5
alcohols									
methanol	28	9.4							
ethanol	65	18.2							
1-propanol	86	29.3							
2-propanol	95	48.0							
1-butanol	92	21.8							
1-hexanol	94	15.5							
aromatics									
benzene	86	NA					6	43.7	54.3
toluene	90	NA					19	81.8	89.2
chlorinated solvents									
1,2-dichloroethane							1.0	11.4	35
cis-1,2-dichloroethene							1.0	37.1	23.5
1,1,1-trichloroethane							32.6	70	95.2
1,1,2-trichloroethane							3.0	33.8	55.6
trichloroethylene							13	74.3	59.3
tetrachloroethylene							48	95.6	96.9
pesticides									
atrazine			99.0	89.6	88.9	81.2			
triadimefon			82.9	78.5	NA	58.1			

petrochemicals									
formaldehyde			27.4	30.8	18.6	16.4			
1,2-ethanediol			56.9	62.3	50.1	38.4			
2-butanone			54.2	60.7	77.6	65.1			
ethyl acetate			65.7	75.1	55.3	45.5			
phenols									
phenol	92	0							
4-ethyl phenol	96	NA							
4-isopropyl phenol	98.4	35					19.5	80.5	97.7
reference	163	163	161	161	161	161	152	182	162

Table 4. **Pretreatment Methods to Prevent Fouling in RO**[a]

Fouling material	Pretreatment method
biological fouling	chlorination ozonation uv light UF NF
colloids	coagulation–filtration UF
scaling	acid treatment antiscale agents (SHMP) chelating agents (edta) sand filtration NF
organics	coagulation–filtration activated carbon oxidation UF NF
metal oxides	proper materials acid treatment UF NF
proteins	MF UF
suspended solids	cartridge filtration screen filters MF UF

[a] See Refs. 27, 172–174.

Table 5. **Membrane Cleaning Methods in Reverse Osmosis**

physical cleaning methods	sponge ball
	back pressure flushing
	vibration
chemical cleaning methods	edta, chelating agent
	surfactants
	acids
	sodium dithionate–iron-containing scales